

A New X-ray Analysis of the Open Cluster Blanco 1 Using Wide-field BVI_c Photometric¹ and Proper Motion Surveys

P. A. Cargile¹, D. J. James^{1,2}, and I. Platais³

ABSTRACT

We perform a new analysis of the extant ROSAT and XMM-Newton X-ray surveys of the southern open cluster Blanco 1, utilizing new BVI_c photometric and proper motion data sets. In our study, we match optical counterparts to 47 X-ray sources associated with Blanco 1 cluster members, 6 of which were listed in previous X-ray studies as cluster nonmembers. Our new catalog of optical counterparts to X-ray sources clearly traces out the Blanco 1 main sequence in a color-magnitude diagram, extending from early G to mid-M spectral types. Additionally, we derive new X-ray luminosities as well as ratios of X-ray to bolometric luminosities for confirmed cluster members. We compare these X-ray properties to other young open clusters, including the coeval Pleiades cluster, to investigate the relationship between age and X-ray activity. We find that stars in Blanco 1 generally exhibit X-ray properties similar to those of other open clusters, namely increasing L_x/L_{bol} with reducing mass for earlier-type stars, and a saturation limit of L_x/L_{bol} at a magnitude of 10^{-3} for stars with $V - I_c \gtrsim 1.25$. More generally, the X-ray detected stars in Blanco 1 have X-ray emission magnitudes that agree with the overall trends seen in the other young clusters. We observe that X-ray emission decays as a function of age and the rate of this decay is mass dependent. Specifically, for higher mass stars, the trend is Skumanich like (i.e. $L_x/L_{bol} \propto \text{age}^{-1/2}$); however, as one goes to lower masses the magnitude of X-ray emission becomes less of a function of age. In fact, for the lowest mass stars (M-type), there is no observable reduction in X-ray production during the first ~ 1 Gyr of their lives. However, due to a lack of sensitivity to low X-ray fluxes, there may exist M-type stars that have less than saturated levels of X-ray flux which are not included in our study. In a direct comparison of Blanco 1 to the Pleiades open cluster, members of both clusters have similar X-ray characteristics; however, there does appear to be some discrepancies in the distribution of L_x/L_{bol} as a function of color that may be related to scatter seen in the Pleiades CMD. Moreover, previous comparisons of this nature for Blanco 1 were not possible due to the reliance on photographic photometry. This is where the power of precise, homogeneous, and standardized CCD photometry allows for a high fidelity, detailed study of the X-ray properties of stars in Blanco 1, as well as a thorough comparison of Blanco 1 to other well-studied open clusters.

Subject headings: open clusters and associations: general — open clusters and associations: individual (Blanco 1) — stars: activity — stars: evolution — X-rays: stars

¹Department of Physics and Astronomy, Vanderbilt University, Nashville, TN 37235, USA, p.cargile@vanderbilt.edu

²Physics and Astronomy Department, University of Hawai'i at Hilo, Hilo, HI 96720, USA

³Department of Physics and Astronomy, Johns Hopkins University, Baltimore, MD, 21218, USA

¹Based on observations made with the Small- and Medium-Aperture Research Telescope System (SMARTS) at the Cerro Tololo Inter-American Observatory.

1. Introduction

X-ray emission is a common characteristic among young, main-sequence, solar-type stars. Magnetic fields, produced through a solar-type, magneto-hydrodynamical dynamo process (Parker 1955, 1979), are able to confine and heat plasma to extreme temperatures ($\geq 10^6$ K) in stellar coronae. This highly energized plasma is responsible for the production of the observed X-ray emission from solar-type stars (Rosner et al. 1978; Sams et al. 1992).

Because this plasma heating is highly dependent on the magnetic fields produced by a rotation-induced dynamo, there is a strong, causal relationship between stellar rotation and magnetic field production, and hence induced magnetic activity (e.g., X-rays). In fact, the efficiency of the stellar dynamo is related to both the rotation period, P , and the convective turnover time in the convection zone, τ_c , through the Rossby number ($R_o = P/\tau_c$). Thus for stars with identical rotation periods, we expect increasing magnetic flux levels for stars having increasing τ_c (i.e. decreasing stellar mass) due to a more efficient dynamo. Of course, for decreasing stellar mass, the amount of magnetic flux threading the stellar surface is itself a decreasing function of stellar radius.

Observationally, this framework has proved to be correct, with a positive correlation existing between coronal emission and rotation rate (or Rossby number). For the most part, faster rotating, or lower Rossby number, solar-type stars have higher X-ray luminosities compared with stars with slower rotation rates, or higher Rossby number (e.g. Pallavicini et al. 1981; Vilhu & Walter 1987; Hempelmann et al. 1995). However, observations of more rapidly rotating stars (or those with lower Rossby numbers) are suggestive of a scenario where the dynamo process, or the magnetic heating rate, does not continue increasing without limit and appears to saturate. The data unequivocally show that for late-type stars rotating above $\simeq 15 - 20$ km s $^{-1}$, or for M-dwarfs more like $\simeq 5-8$ km s $^{-1}$, a saturation plateau of maximal coronal X-ray luminosity occurs at the level of 0.1 % of the stellar bolometric luminosity ($L_X/L_{bol} \sim 10^{-3}$; Vilhu & Walter 1987; Stauffer et al. 1994; James et al. 2000). These X-ray characteristics are readily seen in observations of relatively young (≤ 1 Gyr) Galactic open clusters.

Open clusters, being natural samples of stars with the same age, distance, composition, and environmental formation conditions, have long been considered powerful laboratories to test the models of stellar formation and evolution in our Galaxy. Through the study of large numbers of open clusters at several different ages, the complex, interdependent roles of rotation, age, composition, mass, and initial conditions play in determining the levels of X-ray emission from solar-type stars can be investigated.

Blanco 1 is a relatively nearby, young open cluster (250 pc, 60–100 Myr; WEBDA open clusters database²) that is of considerable scientific interest due to its high Galactic latitude ($b = -79^\circ$) and comparable age to the well studied Pleiades open cluster ($\sim 80 - 120$ Myr; Meynet et al. 1993, $[Fe/H] = -0.034 \pm 0.024$; Boesgaard & Friel 1990). Considerable interest in the cluster has been driven by its reported metal-rich nature ($[Fe/H] = +0.23$; Edvardsson et al. 1995), although a more recent, self consistent determination now makes the cluster of near-solar composition ($[Fe/H] = +0.04 \pm 0.04$; Ford et al. 2005). The combination of the cluster’s systemic velocity ($RV_{sys} = +5.5$ km s $^{-1}$; Mermilliod et al. 2008), its Galactic latitude, and distance below the Galactic plane (~ 250 pc) suggests that, if Blanco 1 has an age of >50 Myr, it should have been created in or near to the Galactic plane. The unusual location of Blanco 1 makes it unique among the well studied, young ($\ll 1$ Gyr) open clusters.

²The WEBDA database, developed by J.-C. Mermilliod, can be found at <http://www.univie.ac.at/webda/>

Blanco 1 contains more than 200 known members spread over $\simeq 3 \times 3 \text{ deg}^2$ on the sky (Jeffries & James 1999; James et al. 2009; Mermilliod et al. 2008; Moraux et al. 2007). Such a wide areal on-sky distribution is challenging for deep and complete photometric surveys. The existing X-ray studies of Blanco 1 (Micela et al. 1999a; Pillitteri et al. 2004) have relied on older, photographic photometry (de Epstein & Epstein 1985) to segregate cluster members from Galactic field stars and background galaxies. Due to the inherent scatter in photographic photometry, especially in the photometric precision of fainter objects (see §2.1), definitive membership status and characteristics of optical counterparts to X-ray sources remain poorly established.

In this paper, we re-analyze the X-ray properties of Blanco 1 using a recent, standardized CCD BVI_c photometric survey of the central $1.6 \times 1.3 \text{ deg}^2$ of Blanco 1. This high fidelity photometric data set, in concert with a new proper motion survey, allows us to determine a well constrained membership catalog with standardized photometry down to $V \sim 17$ (§2). We combine this new catalog with the available ROSAT and XMM-Newton X-ray data to compute accurate X-ray luminosities for those photometric sources identified as cluster members. We utilize our new analysis to examine the X-ray properties of the cluster, including the X-ray luminosity and the ratio of X-ray to bolometric luminosity versus intrinsic color distributions (§3). Furthermore, we compare these X-ray properties to other well studied open clusters at various ages to investigate how these distributions evolve with time (§4).

2. Extant Observations

2.1. Optical Photometry

In order to investigate the photometric membership of Blanco 1, de Epstein & Epstein (1985) performed a large-scale survey of the central 1.5 deg^2 of the cluster, utilizing archival photographic plates, obtained at the El Leoncito Observatory in San Juan, Argentina. They were able to identify some 1500 stellar objects down to a limiting magnitude of $V \simeq 16.5$, which corresponds to a late-K spectral type for the reddening and distance of Blanco 1. These authors claim cluster membership for $\simeq 10\%$ of their sample although, as they themselves note, classification of stars fainter than $V = 12.6$ must be considered “tentative”. This is because they produced a photometric dataset based on a calibration between their photographic magnitude system and the then-existing photoelectric dataset for Blanco 1 stars, which unfortunately must be extrapolated for stars fainter than $V \simeq 12.6$.

In light of the paucity of precise and accurate photometric data for Blanco 1, especially for fainter cluster members, a recent study produced a standardized $UBVI_c$ CCD photometric dataset for the central $1.6 \times 1.3 \text{ deg}^2$ of Blanco 1, centered on RA (2000): $00^h 05^m$; DEC (2000): $-30^\circ 02' 4$. The details of this survey are given in James et al. (2009, hereafter J09); here, we merely outline the most pertinent features of their study. $UBVI_c$ CCD photometric data were taken using the SMARTS 1-m telescope at the Cerro Tololo Inter-American Observatory (CTIO), equipped with the $19' 3 \times 19' 3$ Y4K camera. The photometric catalog contains 1668 stellar objects with a limiting magnitude of $V \simeq 17$. Standardization of their instrumental photometric magnitudes comprised some 60 standard stars nightly, with external errors in transforming instrumental magnitudes onto the standard system of $< 2\%$. Comparison of control field photometric data shows that internal errors of their photometric catalog are better than 0.5% ($V < 16$) and statistical errors are $\leq 1\%$ at $V < 16$.

Figure 1 shows the V_0 versus $(B - V)_0$ and $(V - I_c)_0$ color-magnitude diagrams (CMD) based on this photometry. In our study, to convert to intrinsic magnitudes and colors for the BVI CCD photometry, we assume a distance of 240 parsecs as derived from isochrone modeling in J09, as well as $E(B - V) = 0.016$

and $E(V - I) = 0.02$ taken from an average of published reddening coefficients for Blanco 1 (Epstein 1968; Eggen 1970, 1972; Appenzeller 1975; Perry et al. 1978; de Epstein & Epstein 1985; Westerlund et al. 1988). We note that because Blanco 1 lies significantly out of the Galactic plane, we do not expect differential reddening to be an issue. J09 use a τ^2 isochrone fitting routine, as described in Naylor & Jeffries (2006), to model the main sequence of Blanco 1 with a theoretical isochrone from D’Antona & Mazzitelli (1997). They find a model-dependent distance and age for the cluster of 240 ± 10 parsecs and 80 ± 20 Myr, respectively. This distance estimate agrees with the distance (242 pc) from the revised Hipparcos parallax for Blanco 1 at $\pi=4.14\pm0.17$ mas (van Leeuwen 2007). We note that fainter than $V\sim 15$ mag there is an increased possibility for objects not associated with Blanco 1 to contaminate a photometric membership catalog due to large uncertainties in $B - V$ and $V - I$ (see error bars in Fig. 1). Therefore, it becomes essential to use other membership properties, e.g. proper motions (see §2.3), to determine a high fidelity membership list for the faintest stars in Blanco 1.

2.2. Systematics in Previous Photometry

It is instructive to examine the sets of photometric data used in the analysis of X-ray properties of Blanco 1 members. In Fig. 2a,b, a comparison between the photometry of de Epstein & Epstein (1985) and J09 is plotted. Clearly, for magnitudes greater than $V\sim 12.5$, there is an increasingly large offset between the two catalogs, as well as an increase in the $B - V$ scatter for stars redder than ~ 0.7 . This scatter is at a 1σ level of 0.05 for $B - V > 0.7$. These effects are most likely due to the limitations in photographic-to-photoelectric calibration of the de Epstein & Epstein catalog.

Employing photometric data from poorly standardized catalogs carries with it inherent analysis uncertainties. In the X-ray study of Pillitteri et al. (2004, see §2.4.2), they use GSC-II B and R magnitudes transformed onto a version of the standard $B - V$ color system. If one compares these $B - V$ colors with those of stars in common in the J09 standardized photometric dataset for Blanco 1, a quality control assessment of the GSC-II transformation process can be performed. Plotted in the third panel of Fig. 2 are the results of such a comparison, where a clear systematic offset between the two color systems is apparent. The Pillitteri et al. transformed $B - V$ colors are in fact systematically bluer, by 0.07 magnitudes, than the J09 colors. Moreover, there is also considerable dispersion about the mean offset between the two color systems at the 10% level ($1\sigma = 0.12$). These absolute color calibration problems propagate throughout membership determination through isochrone fitting, as well as any calculations of bolometric luminosity for cataloged cluster members (e.g. determining L_x/L_{bol}). For the purpose of this paper, we employ only the BVI_c data from the J09 survey.

2.3. Proper Motions

The recent astrometric study (Platais et al. 2009) produced a new proper motion catalog for the central 8 deg^2 of Blanco 1. An astrometric solution was deduced from a total of 32 sets of photographic and CCD observations with a time base-line of 40 years, ending in 2007 September. Proper motions and positions were calculated using a variant of the central plate-overlap method (e.g. Herbig & Jones 1981) and the UCAC2 catalog (Zacharias et al. 2004) as a reference frame. The precision of the proper motions, for stars with optimal image properties, is 0.3 mas yr^{-1} . The final catalog contains 6300 objects down to $V\sim 17$, among which, more than 3600 have proper-motion precisions better than 2 mas yr^{-1} .

The formal proper-motion membership probabilities, P_μ , were calculated using the probability definition formulated by Vasilevskis et al. (1958): $P_\mu = \Phi_c / (\Phi_c + \Phi_f)$, where Φ_c is the distribution of cluster stars and Φ_f is the distribution of field star proper motions. The distributions of field and cluster stars in the area of Blanco 1 are derived using the so-called local sample method (Platais et al. 2007). The separation between the cluster and field is convincing for the entire magnitude range. A total of 247 stars have their P_μ greater than 0%. A full description of the reduction and analysis of these new astrometric data is given in Platais et al. (2009).

Our new proper-motion membership probabilities can be used to scrutinize a list of astrometric Blanco 1 members given in Table A.1 of Pillitteri et al. (2003). Considering only those stars with V brighter than ~ 17 , we identified 72 out of 93 objects on this list as cluster members based on new proper motions. Among the common stars, we find 17 stars with $P_\mu=0\%$. Apparently, the accuracy of GSC-II proper motions used by Pillitteri et al. (2003) is not adequate to efficiently eliminate field stars from their sample of cluster stars.

2.4. X-Ray Observations

2.4.1. ROSAT

Micela et al. (1999a, hereafter M99) report the results of two deep exposure (~ 70 ks) ROSAT HRI pointings, bore-sighted on the central region of Blanco 1. The two adjacent $40' \times 40'$ pointings were centered at RA(2000): 00^h02^m8 ; DEC(2000): $-30^\circ00'$ (field 1) and RA(2000): 00^h05^m6 ; DEC(2000): $-30^\circ06'$ (field 2). Identification of X-ray sources detected in these pointings was based upon a point-spread function (PSF) detection algorithm, with a source acceptance threshold chosen such that there is no more than one predicted false source detection per HRI image. This procedure yields a total of 132 X-ray sources from both fields in the 0.1 - 2.4 keV energy band. M99 utilize an X-ray error circle for significantly detected sources of $20''$. In order to derive fluxes for their HRI X-ray sources, M99 derives a count rate to flux conversion factor of 3.2×10^{-11} erg cm $^{-2}$ cnt $^{-1}$ assuming a single temperature Raymond-Smith model for an optically thin plasma with a temperature of 1 keV and a hydrogen column density of $\log(N_H) = 20$.

In order to verify that identified X-ray sources are correlated with Blanco 1 cluster members, M99 employed the de Epstein & Epstein (1985) photometric membership list. They found 42 X-ray sources with optical counterparts, lying in X-ray positional errors circles, as well as having de Epstein & Epstein (1985) optical photometry consistent with being associated with the “apparent” Blanco 1 cluster main sequence. They additionally determined 41 X-ray flux upper limits for other likely cluster members, adjudged from de Epstein & Epstein photometry. However, the de Epstein & Epstein photographic photometry has considerable doubts as to its fidelity (see §2.2). These *must* act to introduce uncertainties into a photometric membership criterion, and thus, such optical/X-ray associations might include several spurious/suspect allocations of X-ray activity to uncertain cluster members.

2.4.2. XMM-Newton

Pillitteri et al. (2004, hereafter P04) report the results arising from a deep exposure (50 ks) XMM-Newton pointing of Blanco 1, centered on the coordinates of the field 1 pointing detailed in the M99 study. The observations were obtained with the EPIC camera system, which has a field of view of $30' \times 30'$. P04 used a PSF detection algorithm for source searching, which yielded a total of 190 X-ray sources detected in

the 0.3 - 5.0 keV band. For XMM-Newton, Jansen et al. (2001) states that the absolute location accuracy for the EPIC instrument XMM-Newton is uncertain up to $4''$. Furthermore, P04 finds the internal precision for the EPIC camera to be $2''.3$ for the Blanco 1 field, thus giving a total positional uncertainty of $6''.3$. Mirroring the M99 study, P04 set a source detection threshold such that no more than one spurious detection was predicted, with a key difference being that a positional error radius for X-ray sources of $13''$ was used. A total of 33 of the 190 XMM-Newton X-ray sources are associated with the same optical counterpart in the M99 X-ray source list. P04 computed count rate to flux conversion factors for the 23 brightest X-ray sources from a detailed low-resolution spectral analysis using a grid of 2-T APEC models with photoelectric absorption. The spectra were found to be best modeled by a lower temperature component of 0.33 keV and an upper temperature component that varied typically from 0.8 to 1.5 keV and a hydrogen column density of $\log(N_H) = 20.5$. The count rate to flux conversions factors for these 23 stars were then averaged to get an overall conversion factor of 5.69×10^{-12} erg cm $^{-2}$ cnt $^{-1}$ for the full XMM-Newton X-ray dataset.

P04 establishes cluster membership for Blanco 1 based on a Pillitteri et al. (2003) photometric and proper motion study. This earlier study uses a photometric selection based upon an R versus $B - R$ CMD, obtained from the second generation of the Guide Star Catalog (GSC-II) photometric data. Their analysis used a somewhat *ad hoc* by-eye selection, based on a region a few magnitudes wide around an assumed main-sequence locus. Furthermore, they refine their selection process by excluding photometric members with proper motion membership probabilities $p \leq 0.8$. This methodology can lead to missing targets because proper motion membership probabilities can be dependent upon stellar magnitudes.

Armed with these membership constraints, P04 selected 93 stars as likely members of Blanco 1. Approximately 40% of these stars (36/93) are optical counterparts to XMM-Newton X-ray sources, including eight previously noted as nonmembers by the M99 study. Of the remaining 154 X-ray sources that were not determined as being Blanco 1 cluster members, 90 sources were found to have optical counterparts detailed in either the USNO-B1, GSC-II, or 2MASS catalogs. The remaining 64 (i.e. 154 total – 90 matched sources) X-ray source detections could not be matched with optical counterparts. They are thus likely to be extra-Galactic background objects, which is hardly surprising given that Blanco 1 lies at high Galactic latitude ($b = -79^\circ$). In investigating the optical/X-ray relationships for Blanco 1, P04 used de Epstein & Epstein $B - V$ for stars also found in the M99 study. As for the rest of the X-ray sources, they used the $B - V$ colors derived from the GSC-II $B - R$. Using these calculated $B - V$ colors which contain significant systematic scatter (see §2.2), introduces uncertainty in the optical/X-ray correlations derived in the P04 paper.

3. Revised Membership of X-ray Sources

In order to determine the proper search radius for identifying optical counterparts in the J09 optical catalog to the M99 ROSAT and P04 XMM-Newton datasets, we employ the method outlined in Jeffries et al. (1997). The procedure estimates the number of real versus spurious matches one should expect in a cross-correlation of an X-ray and optical catalog. This involves modeling the cumulative distribution of the closest match separations for the X-ray sources as the sum of two terms; the cumulative distribution of true correlations and the cumulative number of spurious sources which will increase with separation. For the ROSAT dataset, we determine that a search radius of $16''$, which statistically should have $\sim 2/52$ false counterpart matches, optimizes the number of counterpart matches while minimizing the expected spurious matches. The standard deviation of offsets for matched sources and optical counterparts for a $16''$ search radius is $4''.04$. In a similar fashion, we analyze the XMM-Newton X-ray source matched with the J09 optical catalog. Our analysis showed that a search radius of $6''$ would maximize the number of matches while

decreasing the expected spurious matches to $\sim 1/35$. We find that the standard deviation of offsets for our XMM-Newton matches is $1''.38$.

Using the search radii listed above ($16''$ for ROSAT and $6''$ for XMM-Newton), we matched optical counterparts in the J09 catalog to the X-ray sources published in the surveys of M99 and P04. The results of this matching are given in Table 1. To summarize our findings, in Fig. 3 we plot the J09 optical catalog with the 52 ROSAT and 35 XMM-Newton X-ray sources with optical counterparts identified. Considering only those objects with proper motions consistent with the Blanco 1 membership, we find 41 X-ray sources that were previously identified as members of Blanco 1 by M99 and/or P04, including 24 stars observed by both telescopes. Interestingly, our new CCD photometry and proper motion surveys have allowed us to identify an additional six X-ray sources which were incorrectly classified as nonmembers in the preceding X-ray surveys. Furthermore, based on the new proper motions, we reject three X-ray sources that M99 and P04 previously had identified as cluster members. These objects are likely active field stars or background active galaxies. The fact that these sources might be active galaxies is further supported by Richards et al. (2002) where they find that AGN in the SDSS database, with a wide range of redshifts, are clearly found with approximate colors $0.0 < B - V < 1.25$ and $0.0 < V - Ic < 1.5$ (using SDSS filter to $UBVI_c$ conversions of Smith et al. 2002). The unidentified sources in our X-ray dataset have optical counterparts with colors that fall directly within these AGN color ranges. In Fig. 4, we plot a CMD marking only those X-ray sources that we have determined through proper motions to be cluster members. This demonstrates the power of precision photometric and proper motion data in defining a high fidelity cluster membership catalog.

Of the total 47 X-ray sources we identify as being associated with cluster members, 26 have optical counterparts that are included in spectroscopic surveys of Blanco 1 (Jeffries & James 1999; Mermilliod et al. 2008). These surveys find that all 26 stars are identified as having radial velocities consistent with cluster membership.

Moreover, we note that six optical counterparts in J09 are associated with two separate X-ray sources in M99 and P04. It appears that the XMM-Newton sources that P04 identified as Blanco 1 nonmembers were not matched with the M99 ROSAT X-ray dataset. Using the new proper motions, we subsequently find that three of these six stars are, in fact, cluster members (ZS44, BLX-16, BLX-42), while two (BLX-12 and BLX-15) fell below the proper motion survey’s faintness limit. In Table 2, we list all six sources from M99 and P04 along with the single optical counterparts from J09. To be clear, the X-ray detections listed in Table 2 are associated with the same optical counterpart, which M99 and P04 have identified as two separate X-ray sources. Apparently this is not the case.

3.1. X-Ray Luminosity and L_x/L_{bol} ratio for Blanco 1 members

For cluster members which are optical counterparts to X-ray sources in Blanco 1, we derive their X-ray fluxes and luminosities using the published ROSAT and XMM-Newton X-ray count rates listed in M99 and P04. We convert count rates to fluxes applying the available conversion factors, 3.2×10^{-11} erg cm $^{-2}$ cnt $^{-1}$ for ROSAT and 5.69×10^{-12} erg cm $^{-2}$ cnt $^{-1}$ for XMM-Newton, and derived luminosities using the distance reported in J09, 240 pc. We propagate the uncertainties in flux from the published errors in the count rates. In the conversion from flux uncertainties to errors in X-ray luminosities, we use the distance error given in J09. For a selection of ROSAT X-ray sources that did not have published uncertainties (see Table 2 in M99), we calculate their count rate errors using a linear interpolation of stars having both count rates and uncertainties in the M99 ROSAT survey.

In Fig. 5, we show X-ray luminosity versus intrinsic $B - V$ and $V - I_c$ colors for both ROSAT and XMM-Newton Blanco 1 X-ray sources. We calculate intrinsic colors using $E(B - V) = 0.016$ and $E(V - I) = 0.02$ (see §2.1). Also plotted, and included in Table 3, are the mean X-ray luminosity and their 1σ dispersions found for different spectral-types bins. These spectral bins are determined from color to spectral-type conversions defined in Kenyon & Hartmann (1995). Within the observed dispersion levels, the mean L_x as a function of spectral type in the late F to early M star regime is constant. However, especially in the $V - I_c$ domain where lower mass stars are better represented, there is some evidence for a drop in X-ray luminosity. Empirically, observations of several open clusters support this conclusion (for instance, see §4.2 and references therein).

We plot in Fig. 6 the distance-independent ratio of X-ray to bolometric luminosity as a function of intrinsic $B - V$ and $V - I_c$ colors for Blanco 1 stars having X-ray detections. We note that in Fig. 6, as well as in Fig. 5, the $V - I_c$ color should be preferred for the reddest stars because for values greater than ~ 1.4 , $B - V$ becomes insensitive to changes in stellar mass. In our calculation of the bolometric luminosities, we use the bolometric corrections listed in Johnson (1966) for stars with $V - I < 1.6$ and the formalism given in Monet et al. (1992) for stars with $V - I > 1.6$. A clear increase in L_x/L_{bol} is observed as one goes from F-G to mid-K spectral types in Blanco 1. For spectral types later than K5, at $V - I \approx 1.25$ there is a saturation limit at a L_x/L_{bol} of 10^{-3} , where the X-ray production becomes insensitive to changes in spectral type. The exact cause of this limit has yet to be determined, however several theories have been put forward including limitations on the field generation capacity of the stellar dynamo (Gilman 1983; Vilhu & Walter 1987) and/or due to centrifugal forces on magnetic loops in rapidly rotating stars (Jardine & Unruh 1999; James et al. 2000).

3.2. Short-Term X-ray Variability

Previous X-ray studies, M99 and Pillitteri et al. (2005), have provided in-depth investigations of short-term X-ray variability in Blanco 1. Therefore, here we merely provide a summary of those findings. M99 identified four variable X-ray sources in their ROSAT dataset (ZS38,ZS61,ZS75,ZS76). We identify all four of these objects as proper motion members of Blanco 1. In a follow-up variability study of the P04 XMM-Newton dataset, Pillitteri et al. (2005) found 22 variable X-ray sources. For 9 of these 22 sources we find optical counterparts in the J09 optical catalog, as well as identify them as proper motion members of Blanco 1 (ZS45,ZS46,ZS61,ZS75,ZS76,ZS94,ZS95, and BLX-42).

It has been suggested that X-ray flaring in stellar coronae has a causal relationship to X-ray emission saturation. We find three of the four ROSAT sources and four of the nine XMM-Newton sources showing variability have saturated levels of X-ray emission, where saturation is arbitrarily defined as L_x/L_{bol} above $10^{-3.25}$. In addition, nine ROSAT and/or XMM-Newton sources have saturated X-ray emission levels (ZS35,ZS37,ZS40,ZS42,ZS43,ZS53,ZS71,ZS88 and, ZS115) but were not identified by M99 and/or Pillitteri et al. (2005) as having significant X-ray variability. Assuming that the X-ray variability observed is evidence for flaring events, these statistics do not suggest that there is an intrinsic correlation between X-ray flaring and saturated X-ray emission levels.

3.3. Long-Term X-ray Variability: Comparison of ROSAT and XMM-Newton Data Sets

We cross-correlated the source positions listed in both surveys with a match radius of up to $16''$, as derived by the positional uncertainties in the ROSAT data. This search yields 28 matches for photometrically determined cluster members. For matched sources, we plot in Figs. 7 the X-ray luminosity and the L_x/L_{bol} values for both surveys along with lines representing equality and variations by factors of 0.5 and 2.

First, we note that the lack of any statistically significant systematic offset between the ROSAT and XMM-Newton X-ray luminosities/ L_x/L_{bol} values suggest that, even though the two datasets were observed over different energy bands, the conversion factors used to convert counts to X-ray fluxes were modeled correctly by M99 and P04. The reason for this agreement in X-ray flux over the two different energy bands is primarily due to the fact that the peak intensity of X-rays from Sun-like stars is around 1 keV (Güdel 2004). Furthermore, this agreement provides assurance that our following analysis of X-ray emission from Blanco 1 stars does not suffer from instrumental systematics in the two X-ray datasets.

In order to investigate any possible long-term X-ray variability in Blanco 1, we look at the cluster members with X-ray sources in both ROSAT and XMM-Newton surveys. A time-span of ~ 6 years separates these two surveys. These results suggest that the majority of the Blanco 1 cluster members have not undergone significant long-term X-ray variability. The source ZS43 shows a change in X-ray flux greater than a factor of 2, which is very likely due to the source confusion (see below). The apparent lack of long-term X-ray variability in Blanco 1 F-M dwarfs is in agreement with the ROSAT and XMM-Newton L_x comparison made in Pillitteri et al. (2005), as well as variability studies in other open clusters (e.g. the Pleiades Marino et al. 2003). We note that for ZS76, a known X-ray flaring star (Pillitteri et al. 2005), we have adopted the count-rate of the star during its quiescent state.

As stated above, the ROSAT X-ray flux measurement of ZS43 is significantly different than that of the XMM-Newton measurements. This discrepancy is clearly seen in Fig. 7. A close inspection of the field near ZS43 reveals that another X-ray source, ZS42, lies only $11''.6$ away. The close proximity of these sources may lead to near-neighbor source confusion in the X-ray data, and therefore cause two-fold systematic offsets in the ROSAT and XMM-Newton X-ray fluxes for ZS43. First, due to the large PSF of the ROSAT telescope ($>16''$), the counts for ZS43 in M99 likely includes flux from ZS42, and therefore the X-ray flux would be overestimated. Second, the XMM-Newton PSF is smaller than ROSAT and therefore the background level likely includes counts from ZS42 causing the XMM-Newton X-ray flux to be underestimated. A combination of these two effects could explain the observed offset to the top left of this data point in Fig. 7.

4. X-Ray Production in Blanco 1

4.1. X-ray Activity along the Main Sequence

In the left panel of Fig. 8, the $M_V, V - I$ CMD for Blanco 1 is displayed showing the identified optical counterparts to X-ray sources and color-coded according to their magnitude of L_x/L_{bol} . We use the distance from J09 (240 parsecs) to derive the absolute magnitude for Blanco 1. We find X-ray counterparts to 47 optically-identified cluster members extending from early-F to mid-M spectral types. In Blanco 1, a general trend of increasing L_x/L_{bol} with decreasing mass is seen along the main sequence. Although the PSF of ROSAT and XMM-Newton does not allow for observation of individual stars in known binary systems in Blanco 1, we do observe that photometric binaries of a given mass appear to be more X-ray luminous than their single star counterparts lying on the main sequence. This phenomenon is not unique to Blanco 1, with observations

showing that binaries are typically over-luminous in X-rays when compared to single stars (e.g. Pye et al. 1994; Stern et al. 1995; Makarov 2002).

4.2. Activity-Age Relationship

It is known that there exist a strong causal relationship between X-ray emission and rotation rate in solar-type stars (Pallavicini et al. 1981; Stauffer et al. 1994). The underlining cause of this phenomenon can be understood in terms of greater dynamo-induced magnetic field production with increasing rotation rate (Wilson 1966; Kraft 1967). There is, however, an age effect to be considered. This is because, as solar-type stars age on the main sequence, they are capable of losing angular momentum through a magnetically channeled stellar wind (e.g. Weber & Davis 1967; Mestel 1968; Kawaler 1988; Barnes 2003). Therefore, as stars become older their surface rotation rate decreases, resulting in an associated reduction in dynamo-induced magnetic field production. This is the so-called age-rotation-activity paradigm. This generalized scenario is observed in young open clusters and field stars as decay of magnetic activity and rotation in solar-type stars proportionally to inverse square root of their age (t) (Skumanich 1972).

In an effort to understand the relationship between activity and age in open clusters, we explore the mean X-ray luminosities of Blanco 1 stars in relation to several well studied open clusters of various ages. The results of this analysis are displayed in Fig. 9 (*left panel*) and in Table 4. Two trends in the data are apparent. First, the mean X-ray luminosity of the F/G, K, and M stars decrease as a function of age. Our linear, least-squares fits to the data give a time dependence on X-ray luminosity of $L_x \propto t^{-0.60 \pm 0.01}$, $t^{-0.62 \pm 0.27}$, $t^{-0.30 \pm 0.21}$ for spectral-type ranges of F/G, K, and M, respectively. This can be understood as stars having a less efficient dynamo with age because of stellar spin down. Second, the rate of decay is reduced in the M stars compared to the G and K stars in the surveyed clusters. This characteristic of the data is suggestive of longer spin down time scales for the lowest mass stars.

Similarly, we show in Fig. 9 (*right panel*), and in Table 4, the same cluster dataset as in Fig. 9 (*left panel*), this time substituting the mean L_x/L_{bol} for mean L_x . We also compare a linear fit of the data to Skumanich-type spin down function (i.e. $L_x/L_{bol} \propto t^{-\frac{1}{2}}$). For the Skumanich relation, we assume that on average all spectral types have a saturated X-ray level at an age of ~ 1 Myr. This assumption is consistent with observations of very young open clusters (e.g. Feigelson et al. 2002; Stassun et al. 2004). We find from our best-fit, linear trends that L_x/L_{bol} is proportional to $t^{-0.64 \pm 0.41}$, $t^{-0.34 \pm 0.32}$, $t^{-0.08 \pm 0.26}$ for spectral-type ranges of F/G, K, and M, respectively.

One can see some features in Fig. 9 (*right panel*) that give insight into the activity-age relationship in solar-type stars. Formally, in all three mass regimes L_x/L_{bol} decreases as a function of age. Moreover, the rate of decay of the L_x/L_{bol} with age is mass dependent. The earliest spectral type stars in this sample, F- and G-type stars, appear to have L_x/L_{bol} values which decay in a Skumanich-like manner. These higher mass stars are almost exclusively less X-ray active than the saturation level. K-type stars, however, follow a slower decay law of $\sim t^{-1/3}$. Looking more closely, these stars appear to have at or near saturated levels of X-ray emission for ages less than 100 Myr. In older clusters, K stars exhibit reduced magnitudes of X-ray emission due to their increased level of spin down, compared to their younger (< 100 Myr) counterparts. The M stars have an L_x/L_{bol} evolution with age that is clearly non-Skumanich, and in fact, their magnitudes barely decay at all over the first 1 Gyr of their lives (although, see below). We note that our new Blanco 1 results, in L_x and L_x/L_{bol} , are consistent with the X-ray/age dataset for both younger and older open clusters in the first 10^9 years of stellar evolution.

We must caution the reader that by stating M dwarfs are only observed at or near saturated levels of X-ray emission, we are not implying that all young, low-mass stars ($< 1\text{Gyr}$, M spectral types) have L_x/L_{bol} magnitudes of 10^{-3} . Due to the limiting sensitivities of the ROSAT and XMM-Newton telescopes, the completeness level for X-ray surveys of open clusters decreases with decreasing mass. Therefore, the only X-ray sources observed at the lowest masses are the brightest X-ray sources, i.e. those with saturated levels of X-ray emission. In fact, one can observe this in the Hyades where, due to its proximity to the Sun, a near complete stellar population for the cluster is known down to a very low mass (Reid 1993; Bouvier et al. 2008). In the ROSAT study of the Hyades by Stern et al. (1995), they observed X-ray emission from only 30% of the known M dwarfs in the cluster, as compared to 90% of X-ray activity in the known Hyades G stars. Thus, with the extant X-ray datasets for M dwarfs in young, $< 1\text{Gyr}$, open clusters, we are unable to discriminate between the two scenarios of saturated levels of X-ray emission or sample incompleteness.

Cognizant of some limitations in the existing X-ray datasets, let us continue. In Fig. 10, the L_x/L_{bol} distributions of two other well studied open clusters, NGC 2547 (age $\sim 30\text{ Myr}$) and NGC 2516 (age $\sim 140\text{ Myr}$), are directly compared to that of Blanco 1. The data for NGC 2547 and NGC 2516 are taken from Jeffries et al. (2006) and Pillitteri et al. (2006), respectively. In NGC 2547, we generally see stars exhibiting saturated levels of X-ray emission at an earlier spectral type when compared to Blanco 1, in accordance with age-rotation-activity paradigm expectations. Thus, one would expect to still see rapidly rotating, higher mass stars that exhibit saturated levels of X-rays. In both clusters, almost all stars with $V - I_c \geq 1.25$ have saturated levels of X-ray emission. Therefore, in this mass regime, their ages and angular momentum as judged by X-ray emission are indistinguishable.

A comparison of the X-ray properties in Blanco 1 and NGC 2516 is somewhat less straightforward due to the considerable scatter in the L_x/L_{bol} values for NGC 2516 stars at all masses. For the nonsaturated regime, the majority of Blanco 1 stars lie at or above the L_x/L_{bol} distribution for NGC 2516. Moreover, while for Blanco 1 we judge by eye that saturation sets in at $V - I_c = 1.25 \pm 0.02^3$, in NGC 2516 the nexus appears at a redder intrinsic color, $V - I_c = 1.5$. This finding is in agreement with the age-rotation-activity paradigm, that is, for the older NGC 2516, we expect to observe the point where stars exhibit saturated X-ray emission levels at a redder color (i.e. lower mass) when compared to the younger Blanco 1 open cluster. Finally, for the most part stars in the saturated regime of both Blanco 1 and NGC 2516 are indistinguishable in L_x/L_{bol} versus intrinsic $V - I_c$ space. As we state above, this is most probably a result of flux sensitivity limits for the X-ray studies of these clusters, although the considerable scatter in the X-ray distribution of NGC 2516 clouds the issue somewhat.

4.3. Comparison to the Pleiades

Blanco 1 is oftentimes compared with the Pleiades cluster due to its similar age and metallicity (see §1). Under the umbrella of the activity-rotation-age paradigm, one would expect that the X-ray properties of these two clusters should be similar. In Fig. 11, we plot the L_x/L_{bol} versus photometric color distributions for both clusters. The Pleiades optical and X-ray photometry is taken from the ROSAT studies of Stauffer et al. (1994); Micela et al. (1999b) and references cited therein. The optical photometry for the Pleiades used by these authors is photoelectric where such data are available, and photographic otherwise. We notice in both clusters there are two clear distributions. First, there is an increasing level of L_x/L_{bol} values (more active

³Uncertainty determined from an average $V - I_c$ error for stars along the Blanco 1 main sequence with $V - I_c \sim 1.25$.

stars) as mass decreases for bluer, higher mass stars. Second, there is a plateau-like X-ray saturation for all redder, lower mass stars.

However, there does appear to be a difference between the two clusters in the photometric color (i.e. mass) at which X-ray saturation sets in. This mass appears to be higher for the Pleiades, which by the age-activity relationship would indicate that the Pleiads have not spun down as much as their Blanco 1 counterparts, and therefore would appear to be younger. This finding does not agree with previous age measurements for the two clusters. For Blanco 1, fitting of the main-sequence gives 80 Myr (J09); for the Pleiades, main sequence fitting gives 100 Myr (Meynet et al. 1993) and the lithium-depletion boundary age is measured to be 125 Myr (Stauffer et al. 1998).

Looking at the CMD for the X-ray sources for Blanco 1 and the Pleiades (Fig. 8), we clearly see that there is significant scatter across the Pleiades main sequence when compared to Blanco 1. The X-ray selected, photometric members of Blanco 1 appear to trace a much tighter locus in $M_V/V - I_c$ space when compared to the Pleiades cluster. Assuming that each X-ray identified Pleiad is a *bona fide* member of the cluster, only three possibilities can explain this phenomenon. First, the photometric spread on the main sequence is real. Second, the quality of the photometry is insufficient to define a tight main-sequence locus. Finally, differential reddening across the cluster is artificially introducing photometric scatter in the reddening-free $M_V/(V - I_c)_0$ plane. One or all of these factors that lead to this scatter may well be contributing to some of the discrepancies seen in the L_x/L_{bol} versus color distributions for Blanco 1 and the Pleiades. We do note that there is a larger number of sources identified in the Pleiades studies; therefore, the probability increases for including nonmembers in these datasets which coincidentally satisfy the criteria used for selection of cluster membership.

Much of the possible confusion in this discussion of age and X-ray activity at the onset of X-ray saturation in the Blanco 1 and Pleiades clusters centers upon the late F to early K stars ($0.6 < B - V < 0.9$; $0.5 < V - I_c < 1.1$). The morphology of these stars in the L_x/L_{bol} versus intrinsic color plane appears unusual (see Fig. 11), with a clump of apparently saturated stars lying considerably above (up to an order of magnitude) the general trend of increasing L_x/L_{bol} versus intrinsic color (especially in $B - V$ space). At the present time, with the available data, we cannot adequately explain this phenomenon.

5. Summary

Being young (80 Myr), nearby (240 pc), and having a high Galactic latitude ($b = -79^\circ$), the open cluster Blanco 1 presents itself as a valuable laboratory in which to study early stellar evolution. Here, we present a new analysis of the optical/X-ray properties for stars in Blanco 1 using the two extant X-ray surveys (M99 and P04) and a recent standardized BVI_c photometric catalog (J09); membership selection of this cluster is based on newly derived proper motions. We find optical counterparts to 47 X-ray sources in the cluster. We note that six of these sources were misidentified as cluster nonmembers by previous X-ray studies. In our analysis, we derive new L_x and L_x/L_{bol} values for cluster members and compare the distribution of these parameters to other well studied open clusters. We find that the X-ray properties of Blanco 1 stars are in general agreement with those predicted by the age-rotation-activity paradigm. However, there is a disagreement between the distribution of L_x/L_{bol} as a function of $B - V$ and $V - I_c$ color for Blanco 1 and the similar age Pleiades open cluster. This may be the result of large scatter seen in the color-magnitude diagram of the Pleiades X-ray sources, although the shift of a L_x/L_{bol} saturation onset toward higher masses in the Pleiades appears to be larger than this scatter would imply. We do not find any evidence for significant

long-term X-ray variability in the Blanco 1 cluster members.

Existing X-ray datasets (M99,P04) for Blanco 1, especially for objects fainter than a $V \sim 12$, suffer from their reliance on photographic photometry. The analysis of the X-ray properties of Blanco 1 that we present in this manuscript supersedes these earlier analyses because our new study is founded upon a wide-field, high-quality, homogeneous optical photometric dataset, which crucially, we demonstrate is of high internal self-consistency. This property of the accompanying BVI_c photometry allows us to describe the X-ray characteristics of stars in Blanco 1 as a function of mass, without some of the ambiguities affecting the earlier studies.

As evidence of the power of this new standardized photometric dataset, the X-ray detected, proper motion members of Blanco 1 trace out a tight, low-dispersion main sequence, whereas in contrast the Pleiades cluster shows a much higher level of photometric scatter. We also observe that the absolute level of X-ray emission, as given by L_x/L_{bol} , changes along the Blanco 1 main sequence, thus clearly showing that X-ray production in Blanco 1 is mass dependent.

Looking more globally at the connatural relationship between stellar mass, X-ray production, and age, we observe that X-ray production from the stars in Blanco 1 follows very distinct trends seen in other open clusters. Namely, X-ray emission decays as a function of age, and this decay is mass dependent. G-type stars of all ages have X-ray emission that decays with a Skumanich-like trend. However, as one looks at lower mass stars, X-ray emission become less of a function of stellar age. In fact, for the lowest mass (M-type) stars, there is no observable evidence for the reduction of X-ray emission during the first 1 Gyr of their lives, however, due to the limiting flux sensitivities of the ROSAT and XMM-Newton datasets, we are probably not able to detect M-dwarf stars with less than saturated levels of X-ray emission.

We cordially thank J.-C. Mermilliod for his many years of service to the field of astronomy and to the study of open cluster, including his valuable contribution to this paper on Blanco 1. We recognize support for P.A.C. and D.J.J. from the National Science Foundation Career Grant AST-0349075 (P.I. Stassun, K. G.). I. P. gratefully acknowledges support from the National Science Foundation through grant AST 04-06689 to Johns Hopkins University. Dr. Kelly Holley-Bockelmann and an anonymous referee are thankfully acknowledged for input on this manuscript. We also gratefully acknowledge the staff at CTIO and the SMARTS Consortium. The Cerro Tololo Inter-American Observatory, and the National Optical Astronomy Observatory, are operated by the Association of Universities for Research in Astronomy, under contract with the National Science Foundation. This research has made use of the SIMBAD database, operated at CDS, Strasbourg, France.

Facilities: ROSAT (), XMM (), CTIO:1.0m ()

REFERENCES

- Appenzeller, I. 1975, A&A, 38, 313
Barnes, S. A. 2003, ApJ, 586, 464
Boesgaard, A. M. & Friel, E. D. 1990, ApJ, 351, 467
Bouvier, J., et al. 2008, A&A, 481, 661
D’Antona, F. & Mazzitelli, I. 1997, Mem. Soc. Astron. Ital., 68, 807

- de Epstein, A. E. A. & Epstein, I. 1985, *AJ*, 90, 1211
- Edvardsson, B., Pettersson, B., Kharrazi, M., & Westerlund, B. 1995, *A&A*, 293, 75
- Eggen, O. J. 1970, *ApJ*, 161, 159
- . 1972, *ApJ*, 173, 63
- Epstein, I. 1968, *AJ*, 73, 556
- Feigelson, E. D., Broos, P., Gaffney, III, J. A., Garmire, G., Hillenbrand, L. A., Pravdo, S. H., Townsley, L., & Tsuboi, Y. 2002, *ApJ*, 574, 258
- Ford, A., Jeffries, R. D., & Smalley, B. 2005, *MNRAS*, 364, 272
- Gilman, P. A. 1983, *ApJS*, 53, 243
- Güdel, M. 2004, *A&A Rev.*, 12, 71
- Hempelmann, A., Schmitt, J. H. M. M., Schultz, M., Ruediger, G., & Stepien, K. 1995, *A&A*, 294, 515
- Herbig, G. H. & Jones, B. F. 1981, *AJ*, 86, 1232
- James, D. J., Deliyannis, C. P., Steinhauer, A., Cargile, P. A., & Platais, I. 2009, *ApJS*, in prep.
- James, D. J., Jardine, M. M., Jeffries, R. D., Randich, S., Collier Cameron, A., & Ferreira, M. 2000, *MNRAS*, 318, 1217
- Jansen, F., et al. 2001, *A&A*, 365, L1
- Jardine, M. & Unruh, Y. C. 1999, *A&A*, 346, 883
- Jeffries, R. D., Evans, P. A., Pye, J. P., & Briggs, K. R. 2006, *MNRAS*, 367, 781
- Jeffries, R. D. & James, D. J. 1999, *ApJ*, 511, 218
- Jeffries, R. D., Thurston, M. R., & Pye, J. P. 1997, *MNRAS*, 287, 350
- Johnson, H. L. 1966, *ARA&A*, 4, 193
- Kawaler, S. D. 1988, *ApJ*, 333, 236
- Kenyon, S. J. & Hartmann, L. 1995, *ApJS*, 101, 117
- Kraft, R. P. 1967, *ApJ*, 150, 551
- Makarov, V. V. 2002, *ApJ*, 576, L61
- Marino, A., Micela, G., Peres, G., & Sciortino, S. 2003, *A&A*, 406, 629
- Mermilliod, J.-C., Platais, I., James, D. J., Grenon, M., & Cargile, P. A. 2008, *A&A*, 485, 95
- Mestel, L. 1968, *MNRAS*, 138, 359
- Meynet, G., Mermilliod, J.-C., & Maeder, A. 1993, *A&AS*, 98, 477
- Micela, G., Sciortino, S., Favata, F., Pallavicini, R., & Pye, J. 1999a, *A&A*, 344, 83

- Micela, G., et al. 1999b, *A&A*, 341, 751
- Monet, D. G., Dahn, C. C., Vrba, F. J., Harris, H. C., Pier, J. R., Luginbuhl, C. B., & Ables, H. D. 1992, *AJ*, 103, 638
- Moraux, E., Bouvier, J., Stauffer, J. R., Barrado y Navascués, D., & Cuillandre, J.-C. 2007, *A&A*, 471, 499
- Naylor, T. & Jeffries, R. D. 2006, *MNRAS*, 373, 1251
- Pallavicini, R., Golub, L., Rosner, R., Vaiana, G. S., Ayres, T., & Linsky, J. L. 1981, *ApJ*, 248, 279
- Parker, E. N. 1955, *ApJ*, 122, 293
- . 1979, *Cosmical magnetic fields: Their origin and their activity* (Oxford: Clarendon)
- Patten, B. M. & Simon, T. 1996, *ApJS*, 106, 489
- Perry, C. L., Walter, D. K., & Crawford, D. L. 1978, *PASP*, 90, 81
- Perryman, M. A. C., et al. 1998, *A&A*, 331, 81
- Pillitteri, I., Micela, G., Damiani, F., & Sciortino, S. 2006, *A&A*, 450, 993
- Pillitteri, I., Micela, G., Reale, F., & Sciortino, S. 2005, *A&A*, 430, 155
- Pillitteri, I., Micela, G., Sciortino, S., Damiani, F., & Harnden, Jr., F. R. 2004, *A&A*, 421, 175
- Pillitteri, I., Micela, G., Sciortino, S., & Favata, F. 2003, *A&A*, 399, 919
- Platais, I., Girard, T. M., Vieira, K., Castillo, D., Mermilliod, J.-C., James, D. J., & Cargile, P. A. 2009, in prep.
- Platais, I., Melo, C., Mermilliod, J.-C., Kozhurina-Platais, V., Fulbright, J. P., Méndez, R. A., Altmann, M., & Sperauskas, J. 2007, *A&A*, 461, 509
- Prosser, C. F., Stauffer, J. R., Caillault, J.-P., Balachandran, S., Stern, R. A., & Randich, S. 1995, *AJ*, 110, 1229
- Pye, J. P., Hodgkin, S. T., Stern, R. A., & Stauffer, J. R. 1994, *MNRAS*, 266, 798
- Randich, S. & Schmitt, J. H. M. M. 1995, *A&A*, 298, 115
- Randich, S., Schmitt, J. H. M. M., Prosser, C. F., & Stauffer, J. R. 1995, *A&A*, 300, 134
- . 1996, *A&A*, 305, 785
- Reid, N. 1993, *MNRAS*, 265, 785
- Richards, G. T., et al. 2002, *AJ*, 123, 2945
- Rosner, R., Tucker, W. H., & Vaiana, G. S. 1978, *ApJ*, 220, 643
- Sams, III, B. J., Golub, L., & Weiss, N. O. 1992, *ApJ*, 399, 313
- Skumanich, A. 1972, *ApJ*, 171, 565
- Smith, J. A., et al. 2002, *AJ*, 123, 2121

- Soderblom, D. R., Nelan, E., Benedict, G. F., McArthur, B., Ramirez, I., Spiesman, W., & Jones, B. F. 2005, *AJ*, 129, 1616
- Stassun, K. G., Ardila, D. R., Barsony, M., Basri, G., & Mathieu, R. D. 2004, *AJ*, 127, 3537
- Stauffer, J. R., Caillault, J.-P., Gagne, M., Prosser, C. F., & Hartmann, L. W. 1994, *ApJS*, 91, 625
- Stauffer, J. R., Schultz, G., & Kirkpatrick, J. D. 1998, *ApJ*, 499, L199+
- Stern, R. A., Schmitt, J. H. M. M., & Kahabka, P. T. 1995, *ApJ*, 448, 683
- van Leeuwen, F. 2007, *Hipparcos, the New Reduction of the Raw Data* (Dordrecht: Springer)
- Vasilevskis, S., Klemola, A., & Preston, G. 1958, *AJ*, 63, 387
- Vilhu, O. & Walter, F. M. 1987, *ApJ*, 321, 958
- Weber, E. J. & Davis, L. J. 1967, *ApJ*, 148, 217
- Westerlund, B. E., Lundgren, K., Petterson, B., Garnier, R., & Breysacher, J. 1988, *A&AS*, 76, 101
- Wilson, O. C. 1966, *ApJ*, 144, 695
- Zacharias, N., Urban, S. E., Zacharias, M. I., Wycoff, G. L., Hall, D. M., Monet, D. G., & Rafferty, T. J. 2004, *AJ*, 127, 3043

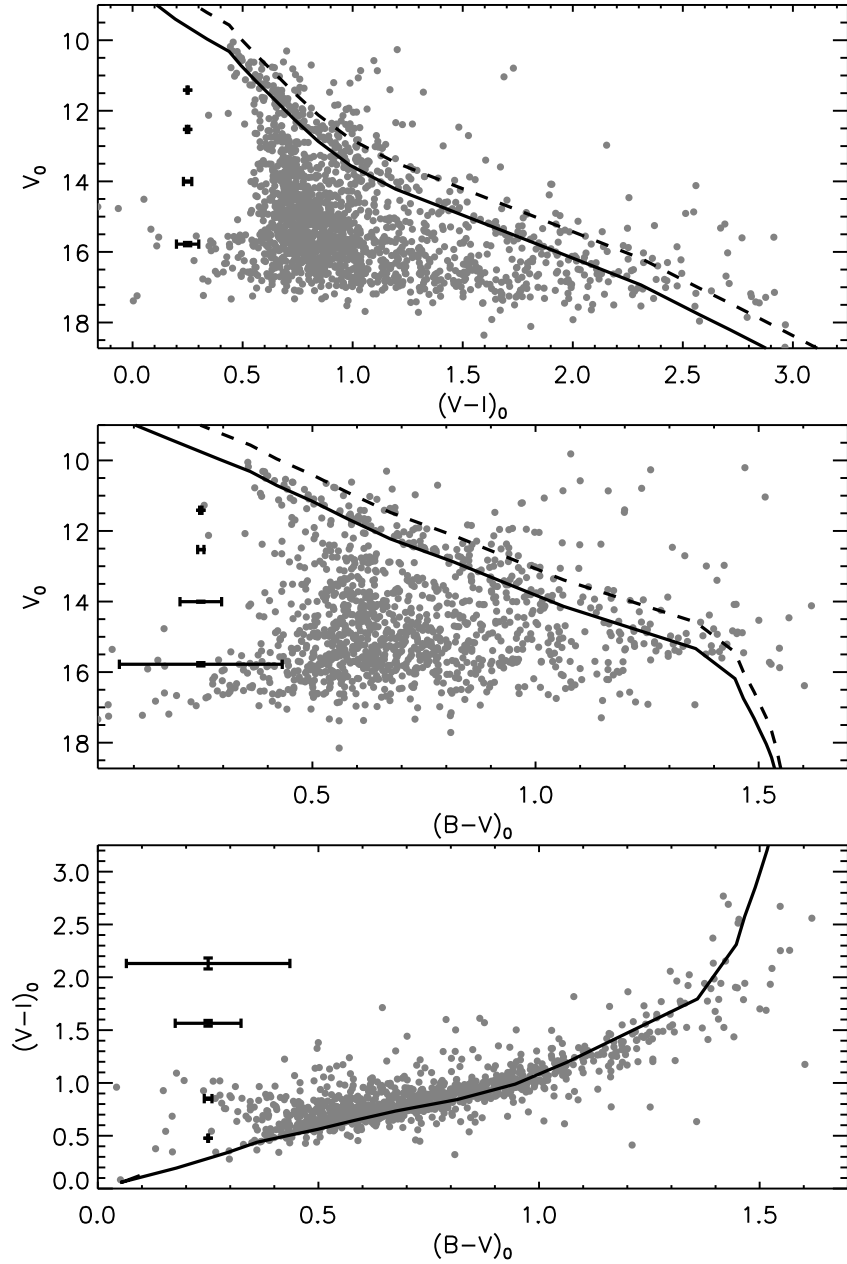


Fig. 1.— Intrinsic color-magnitude and color-color diagrams for the full J09 photometric catalog are plotted. An $E(B - V) = 0.016$ and $E(V - I_c) = 0.02$ has been used. We overplot the best-fit D’Antona & Mazzitelli (1997) isochrone from the James et al. (2009) paper (*solid line*), as well as the equal mass binary sequence (*dashed line*). On the left, we plot the average error bars for objects that lie along the main-sequence isochrone.

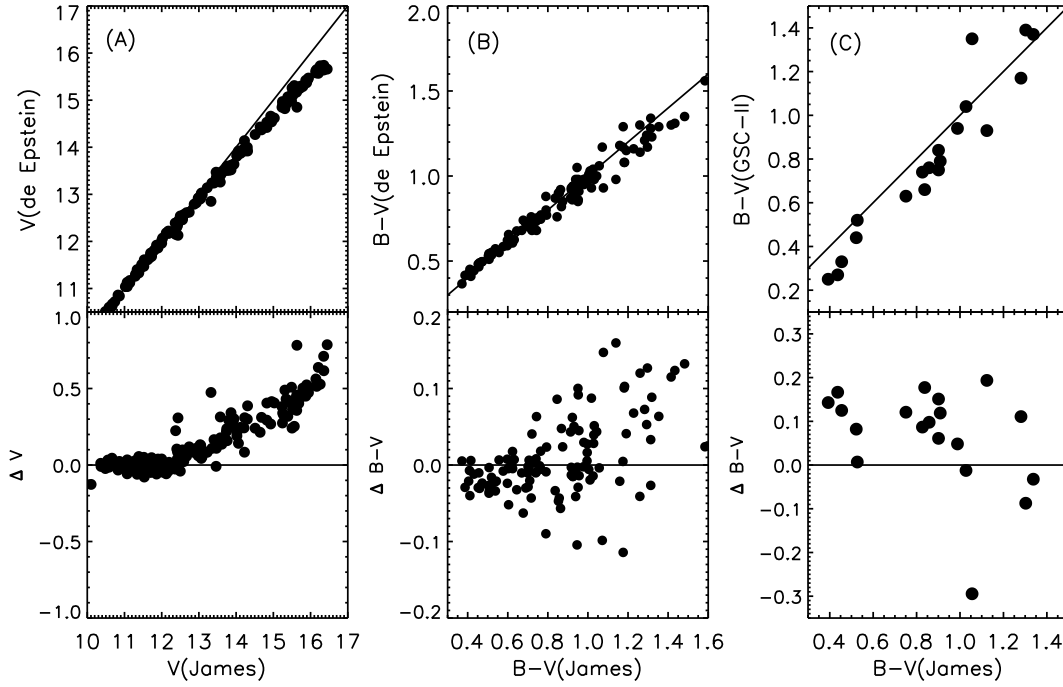


Fig. 2.— V and $B - V$ comparison plots for the de Epstein & Epstein (1985) (A,B) and GSC-II (C) photometric catalogs with the photometry given in J09 are presented. The solid lines indicate equality between the systems, and are not fits to the data.

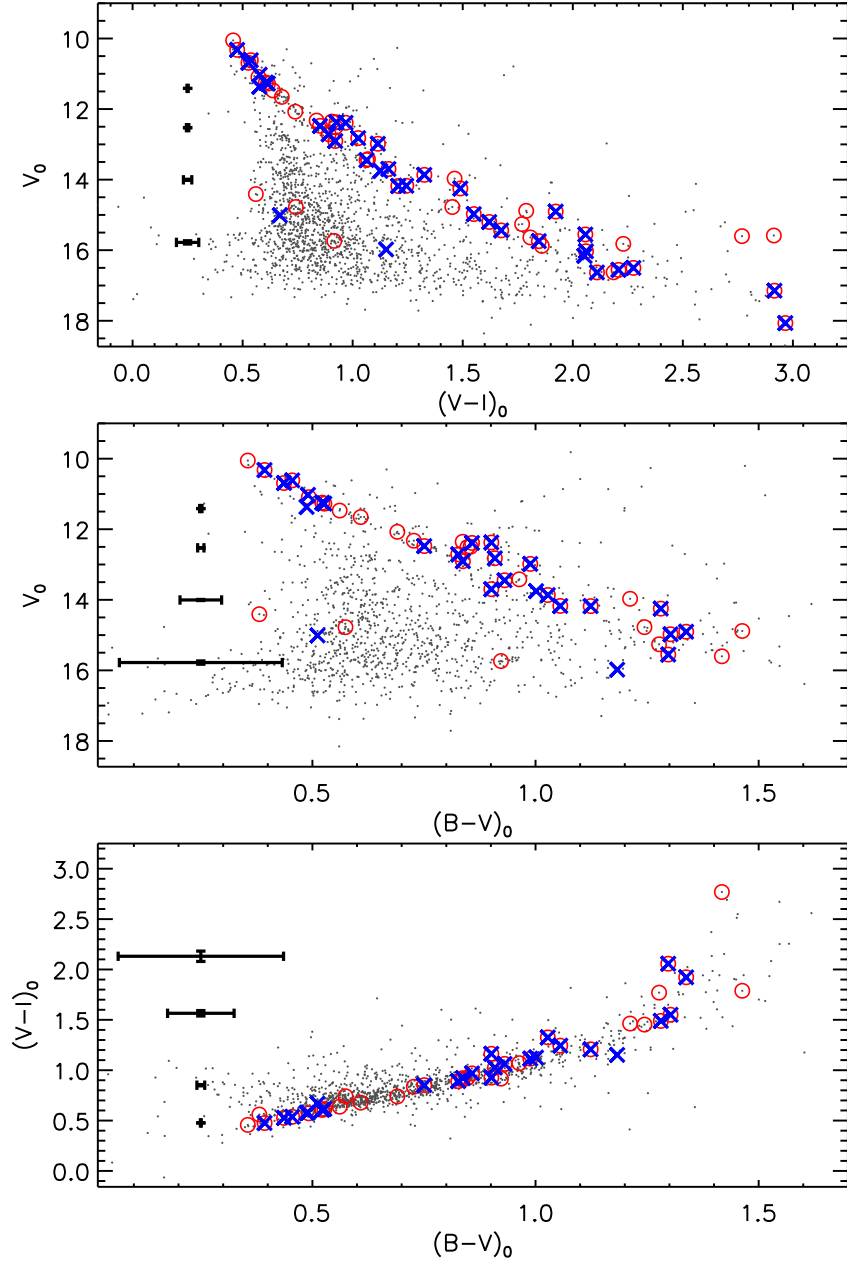


Fig. 3.— Same as Fig. 1 however without the isochrones overplotted. In addition, we identify the optical counterparts to X-ray sources from ROSAT (*red open circles*) and XMM-Newton (*blue crosses*).

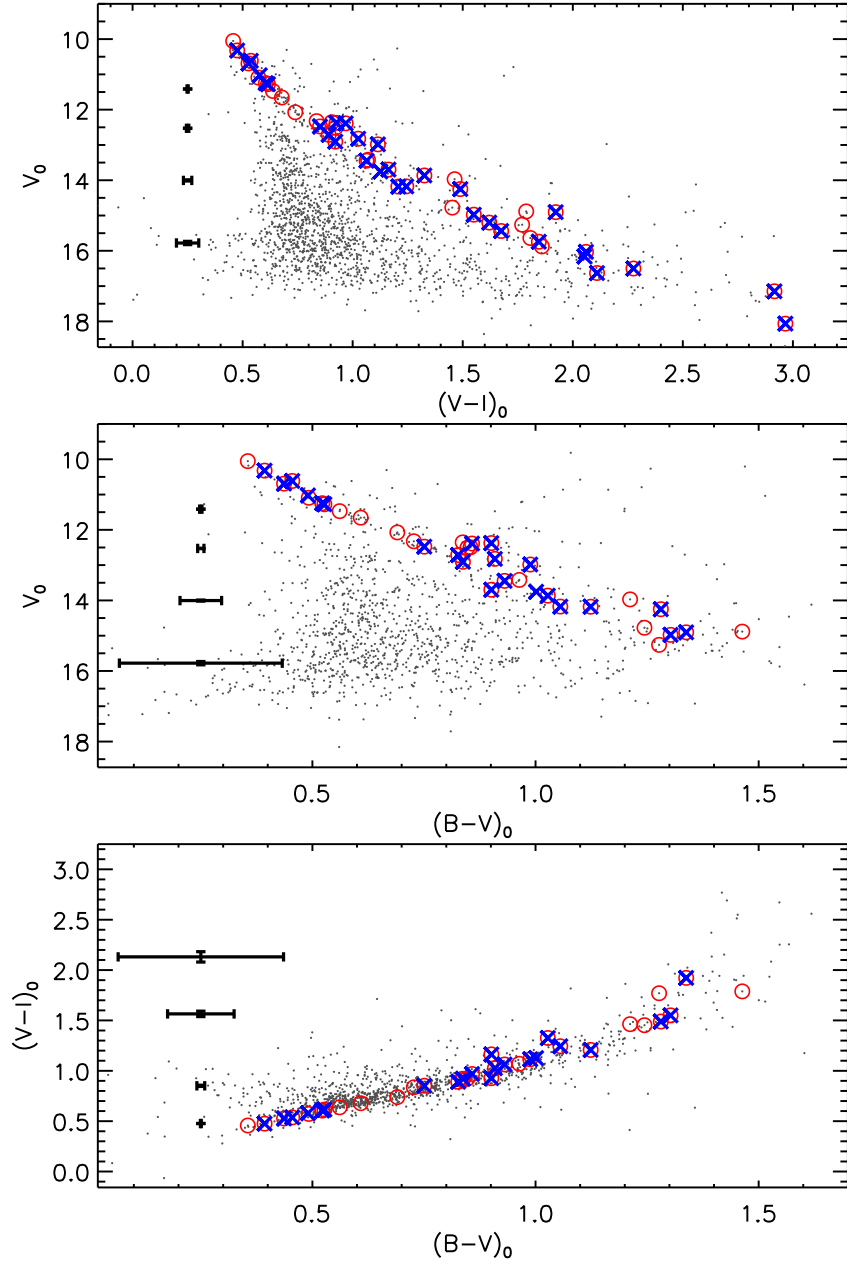


Fig. 4.— Same as Fig. 3, where ROSAT (*red open circles*) and XMM-Newton (*blue crosses*) are identified. However, now only those objects are included that have proper motions consistent with the systemic motion of the cluster.

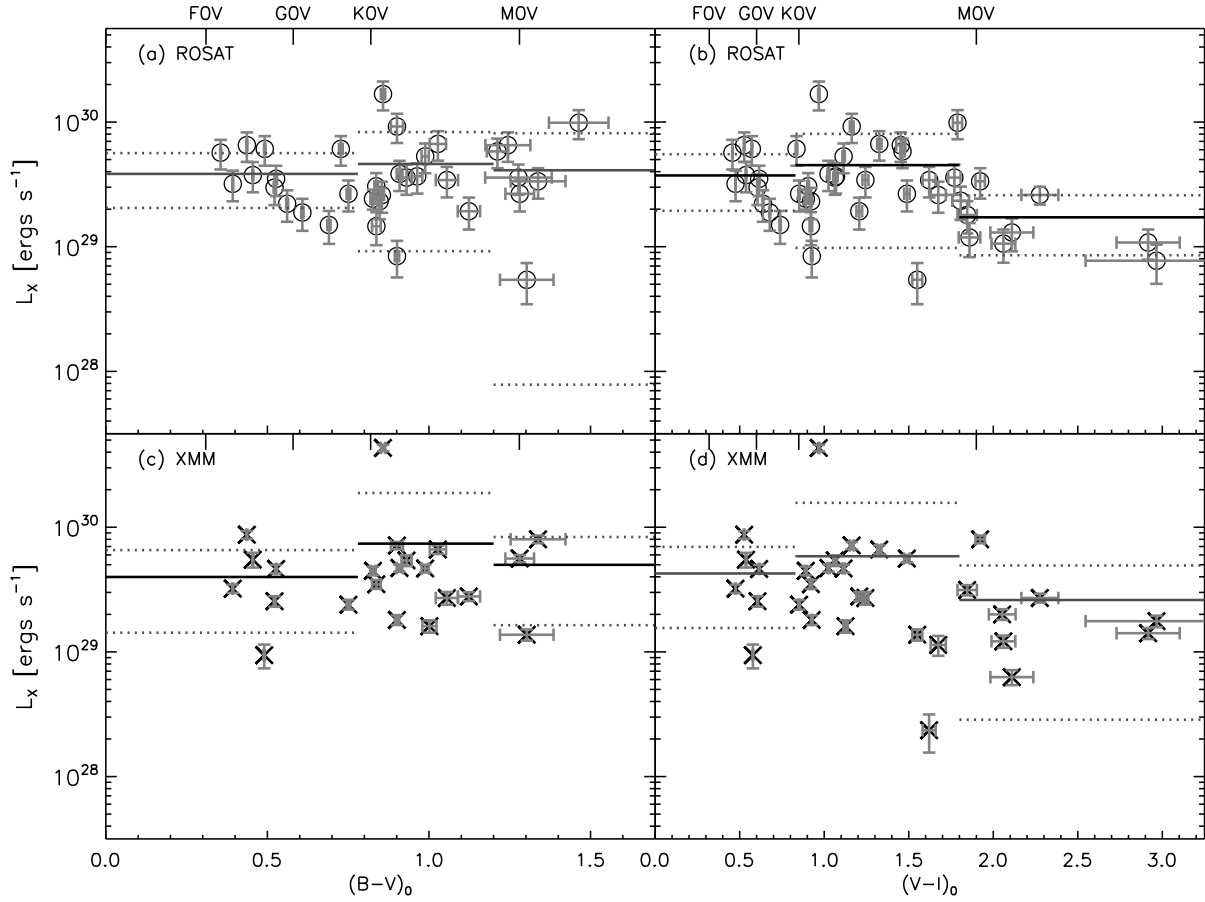


Fig. 5.— X-ray luminosity from ROSAT (*open circles*) and XMM-Newton (*crosses*) as a function of intrinsic $B - V$ and $V - I$ for Blanco 1 cluster members. The solid lines indicate the mean L_x for F & G, K, and M stars, where dotted lines represent 1σ values about these means for each given spectral types.

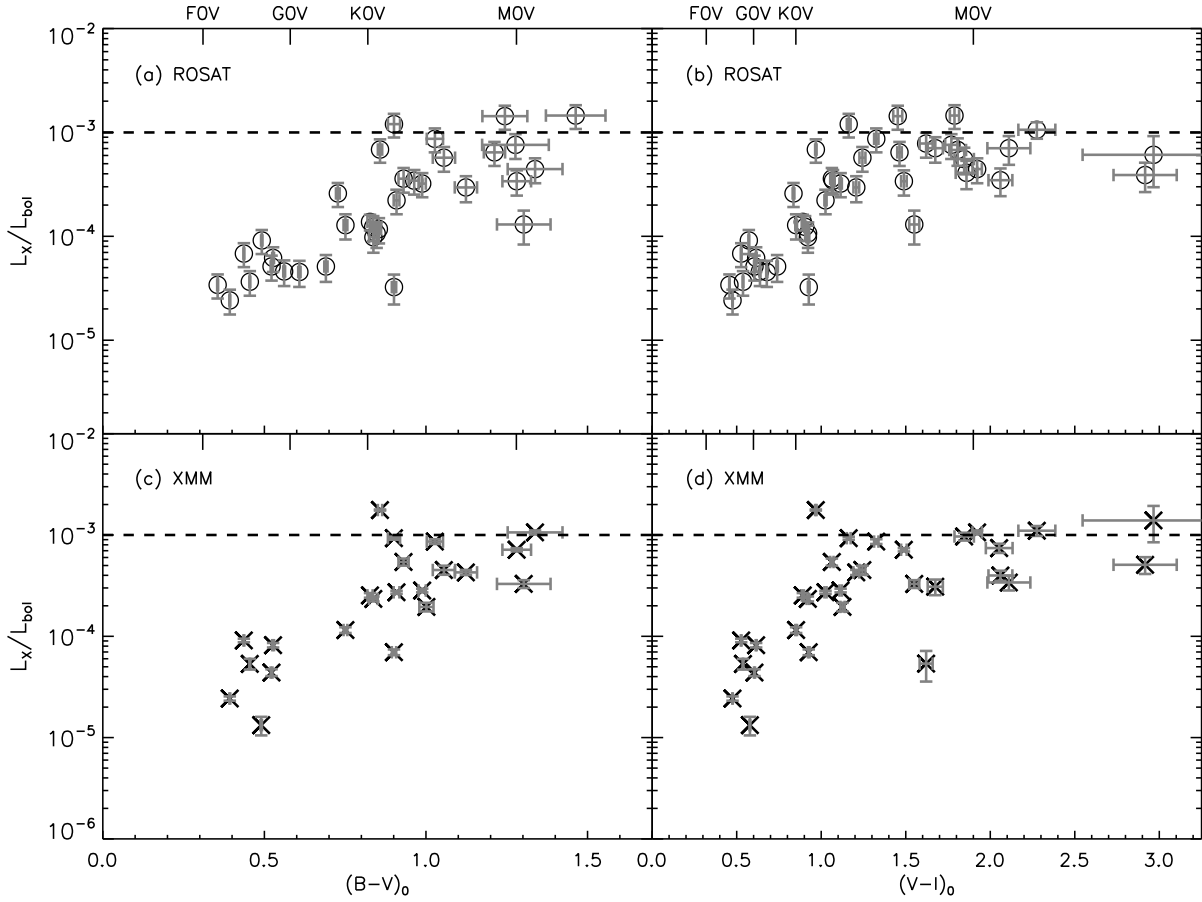


Fig. 6.— Ratio of X-ray to bolometric luminosity plotted as a function of intrinsic color for ROSAT (*open circles*) and XMM-Newton (*crosses*) sources in Blanco 1. The dashed line marks the level at which X-ray luminosity reaches 0.1 % of the bolometric luminosity, which is canonically known as X-ray saturation (e.g. Stauffer et al. 1994).

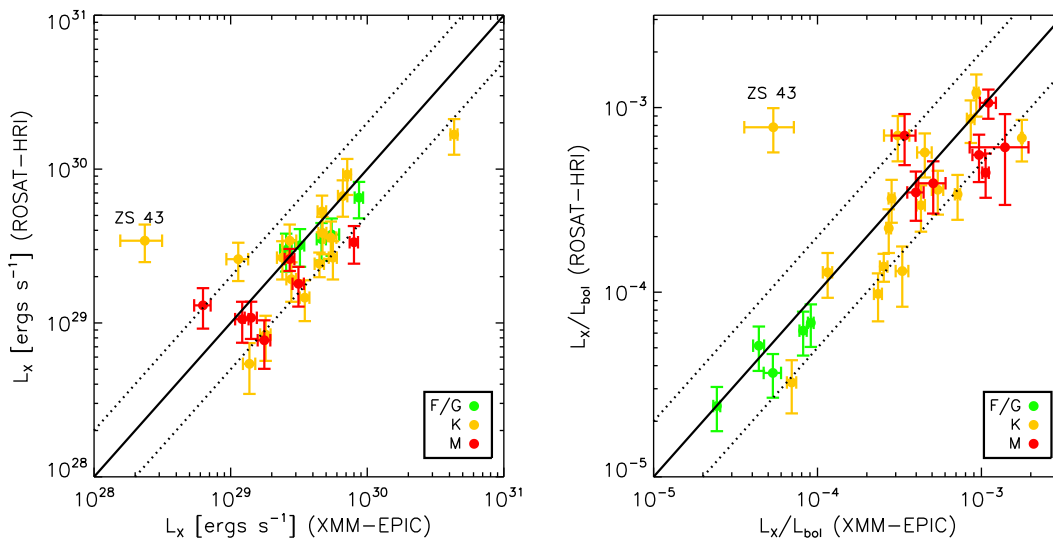


Fig. 7.— Comparison of X-ray luminosity (*left*) and X-ray to bolometric luminosity (*right*) for the 28 cluster members observed with both ROSAT and XMM-Newton, separated by ~ 6 yr. The *solid* lines marks equality between measurements, whereas variations by factors of 0.5 and 2.0 (*dotted lines*) are also shown. We also color code these stars according to the different spectral ranges as defined by the colors given in Kenyon & Hartmann (1995). One star (ZS43), that shows significant discordancy between the measurement systems, is identified.

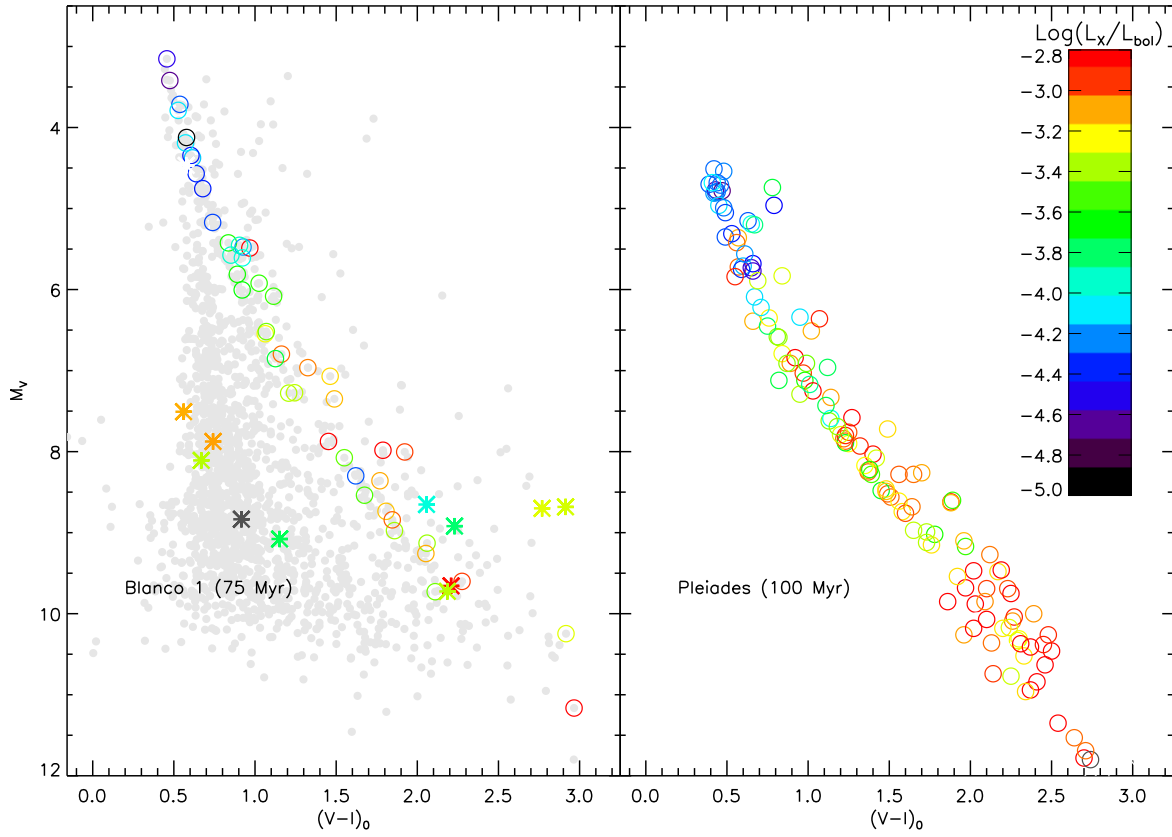


Fig. 8.— Comparison of CMD is shown for Blanco 1 (*left*) and Pleiades (*right*) open clusters, with optical counterparts to X-ray sources identified. The magnitude of the ratio of X-ray to bolometric luminosity, given by the color coding, is shown on the right-hand panel. To derive the absolute magnitude for the two clusters we use 240 (J09) and 133 (Soderblom et al. 2005) parsecs for Blanco 1 and the Pleiades, respectively. For the Blanco 1 cluster, nonmembers are noted with asterisks, and the full photometric catalog is shown in gray.

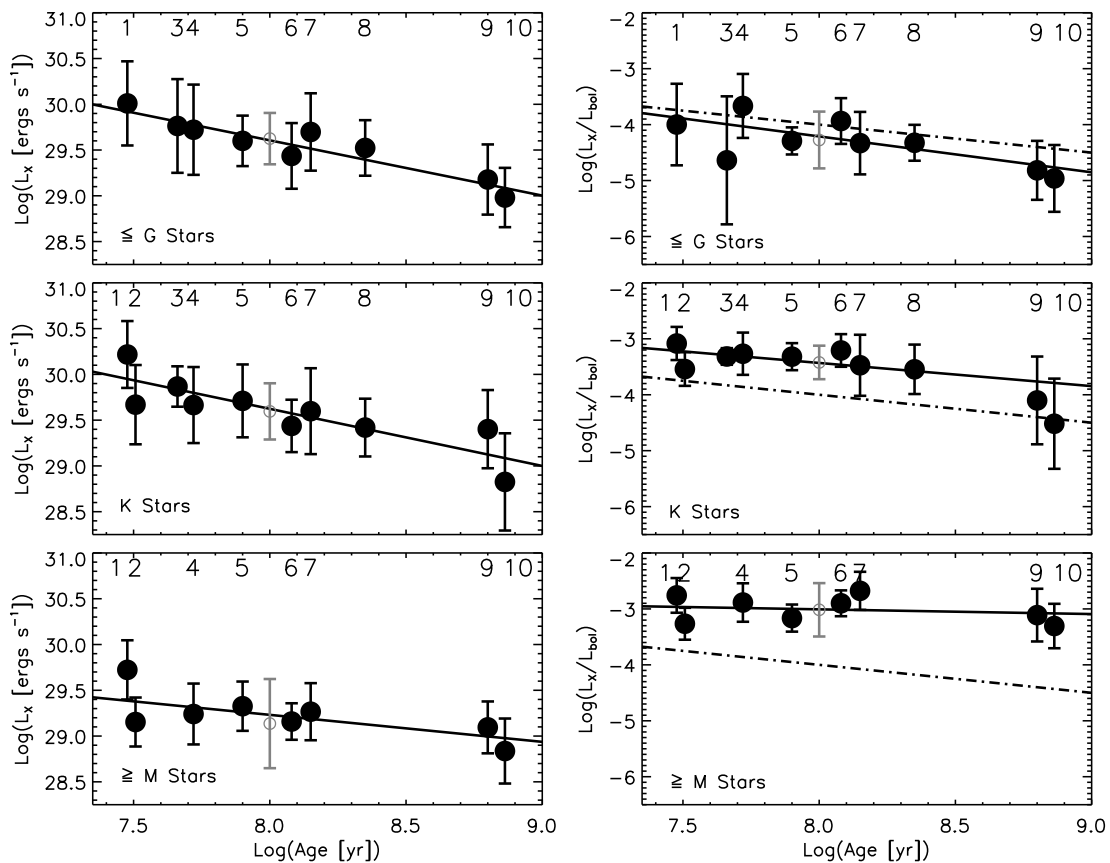


Fig. 9.— Evolution of L_x (left) and L_x/L_{bol} (right) as a function of age is shown for these various open clusters detailed in Table 4, including our new Blanco 1 measurements (5) as well as those derived by P04 (light-font, open circle). Reference numbers (1-10) from Table 4 are shown in the upper part of each panel. Error bars represent the 1σ scatter for the given spectral ranges for each cluster. The solid lines indicate linear, least-squares fits to the cluster data. In the right panel, the dash-dotted lines indicate a Skumanich-like (i.e. $L_x/L_{bol} \sim \text{Age}^{-\frac{1}{2}}$) decay in X-ray emission. The initial conditions for the Skumanich functions are $L_x/L_{bol} = 10^{-3}$ at 1 Myr.

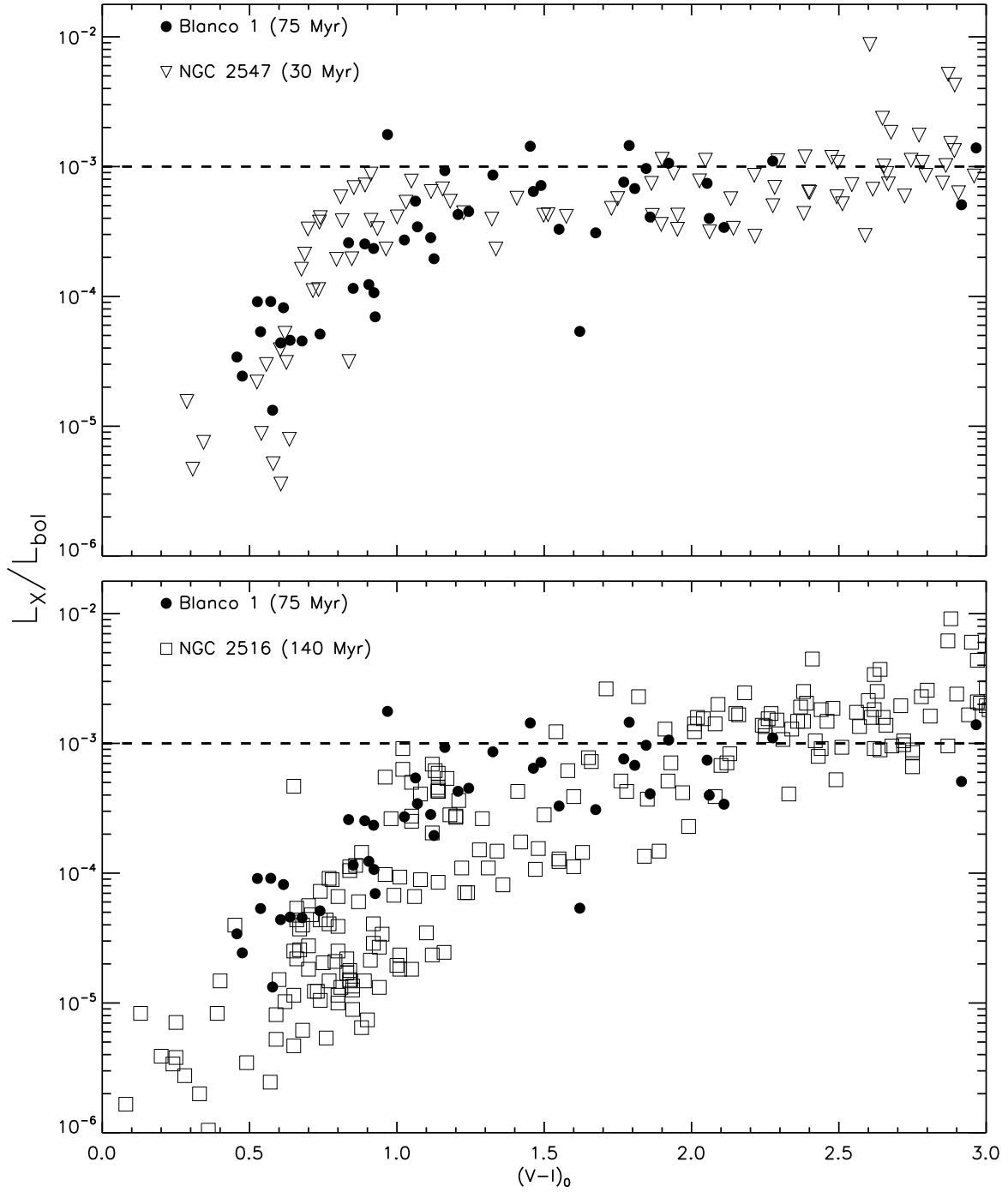


Fig. 10.— L_x/L_{bol} distributions for open clusters NGC 2547 (*triangles*) and NGC 2516 (*squares*) with the Blanco 1 distribution (*solid points*) overplotted. The dashed line denotes a L_x/L_{bol} of 10^{-3} , commonly referred to as the saturation point of X-ray emission.

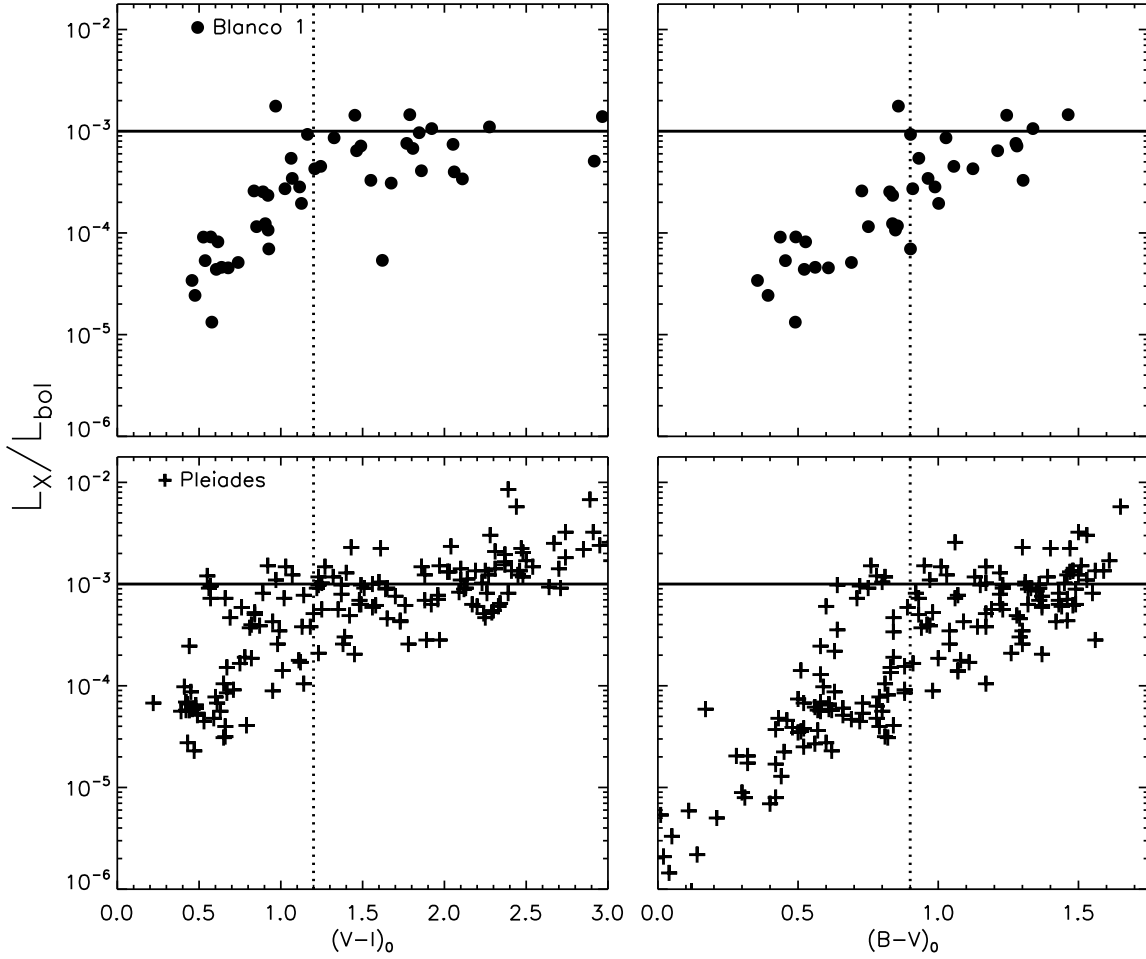


Fig. 11.— A direct comparison of the X-ray to bolometric luminosity distributions for the Blanco 1 (*top*) and Pleiades (*bottom*) open clusters is plotted in intrinsic $V - I_c$ (*left*) and $B - V$ (*right*) space, respectively. The Pleiades optical and X-ray data were taken from Stauffer et al. (1994); Micela et al. (1999b) and references therein. The solid lines represent an observed saturated level of $L_x/L_{bol} = 10^{-3}$. The dotted lines represent a by-eye determination of the onset of saturation in Blanco 1.

Table 1. Blanco 1 X-ray Source Catalog

ID ^a	RA ^b [HH:MM:SS]	DEC ^b [DD:MM:SS]	V_0^c	$(V - I_c)_0^c$	$(B - V)_0^c$	ROSAT [0.1-2.4 keV]		XMM-NEWTON [0.3-5.0 keV]		$\mu_\alpha \cos \delta^e$	μ_δ^e	P_μ^e	P.M. ^e Mem.
						$LogL_x^d$	$Log L_x/L_{bot}$	$LogL_x^d$	$Log L_x/L_{bot}$				
ZS35	00:01:39.85	-30:04:38.4	14.78±0.022	1.45±0.027	1.24±0.070	29.81	-2.84	22.0	1.7	60	Y
ZS58	00:01:46.46	-29:46:38.7	12.32±0.003	0.84±0.005	0.73±0.006	29.78	-3.59	20.8	2.5	86	Y
ZS37	00:01:53.42	-30:06:12.9	15.74±0.052	1.85±0.057	...	29.25	-3.26	29.49	-3.02	22.3	3.0	58	Y
ZS38	00:01:54.44	-30:07:41.8	13.86±0.010	1.33±0.013	1.03±0.025	29.82	-3.06	29.82	-3.07	22.0	2.4	86	Y
ZS40	00:01:56.92	-30:12:07.9	15.44±0.039	1.67±0.045	...	29.41	-3.15	29.05	-3.51	22.7	2.6	54	Y
BLX-7	00:02:00.80	-29:59:17.4	12.71±0.004	0.89±0.006	0.83±0.008	29.38	-3.86	29.65	-3.60	21.5	1.9	80	Y
ZS43	00:02:03.69	-30:10:24.9	15.20±0.033	1.62±0.039	...	29.53	-3.11	28.37	-4.27	22.8	4.0	54	Y
ZS42	00:02:04.21	-30:10:34.4	14.17±0.013	1.24±0.018	1.06±0.035	29.53	-3.24	29.43	-3.35	21.8	3.1	89	Y
BLX-12 [§]	00:02:07.66	-30:04:42.6	18.06±0.414	2.97±0.420	...	28.88	-3.22	29.24	-2.86	NA
ZS44 [§]	00:02:14.69	-29:49:04.2	13.45±0.007	1.06±0.010	0.93±0.016	29.55	-3.45	29.73	-3.27	22.1	3.0	92	Y
ZS45	00:02:18.55	-29:51:08.5	12.91±0.006	0.92±0.008	0.84±0.013	29.16	-4.01	29.54	-3.63	22.1	2.0	84	Y
ZS46	00:02:19.73	-29:56:07.5	14.25±0.014	1.49±0.017	1.28±0.044	29.42	-3.47	29.74	-3.15	20.1	1.5	16	Y
ZS48	00:02:21.63	-30:08:21.6	10.69±0.001	0.53±0.002	0.44±0.001	29.81	-4.17	29.93	-4.04	20.7	3.3	90	Y
BLX-15 [§]	00:02:22.90	-30:02:53.2	17.15±0.184	2.92±0.187	...	29.03	-3.41	29.15	-3.29	NA
BLX-16 [§]	00:02:23.63	-29:50:39.8	16.03±0.066	2.06±0.071	...	29.02	-3.46	29.08	-3.40	19.3	5.6	03	Y
ZS53	00:02:24.26	-30:09:09.0	16.16±0.074	2.05±0.079	29.30	-3.13	20.3	-0.7	01	Y
PMS04-94	00:02:25.48	-29:59:17.6	15.98±0.065	1.15±0.087	1.18±0.195	28.37	-3.76	15.0	20.5	00	N
BLX-17	00:02:25.89	-29:52:39.2	16.56±0.105	2.21±0.111	...	29.04	-3.30	29.45	-2.89	16.8	10.9	00	N
ZS54	00:02:28.19	-30:04:43.5	12.98±0.005	1.11±0.007	0.99±0.011	29.72	-3.49	29.66	-3.55	21.8	2.5	90	Y
ZS61	00:02:34.83	-30:05:25.5	13.70±0.008	1.16±0.011	0.90±0.019	29.96	-2.92	29.85	-3.03	21.3	2.1	80	Y
ZS62 [†]	00:02:35.46	-30:07:02.0	12.48±0.003	0.85±0.005	0.75±0.006	29.42	-3.89	29.37	-3.94	21.2	2.9	93	Y
ZS60 [§]	00:02:41.79	-29:58:53.2	15.55±0.043	2.06±0.046	1.30±0.147	29.10	-3.57	28.70	-3.97	-17.8	-12.0	00	N
PMS04-190	00:02:48.22	-29:46:34.9	13.75±0.009	1.13±0.013	1.00±0.022	29.20	-3.71	20.9	3.2	86	Y
BLX-26	00:02:51.52	-29:54:49.4	16.63±0.119	2.11±0.127	...	29.11	-3.15	28.79	-3.47	18.5	3.1	04	Y
ZS76	00:02:56.38	-30:04:44.8	12.39±0.003	0.97±0.004	0.86±0.007	30.22	-3.16	30.63	-2.75	21.6	3.2	95	Y
BLX-32	00:02:59.65	-29:52:52.2	15.82±0.055	2.23±0.058	...	28.84	-3.79	135.5	81.8	00	N
ZS75	00:03:00.28	-30:03:21.6	12.82±0.004	1.03±0.006	0.91±0.009	29.58	-3.65	29.67	-3.57	21.5	3.9	91	Y
BLX-34	00:03:00.56	-30:15:44.0	15.64±0.044	1.81±0.050	...	29.36	-3.17	21.0	1.6	33	Y
ZS71	00:03:02.95	-29:47:44.1	14.90±0.025	1.92±0.028	1.34±0.085	29.52	-3.35	29.90	-2.97	21.2	3.6	80	Y
ZS88	00:03:06.63	-29:43:11.5	13.97±0.011	1.46±0.014	1.21±0.033	29.76	-3.19	21.1	5.0	45	Y
ZS83 [‡]	00:03:07.09	-30:15:17.1	12.51±0.003	0.92±0.005	0.85±0.007	29.36	-3.97	21.9	2.6	94	Y
ZS84	00:03:10.81	-30:10:49.0	11.28±0.002	0.62±0.003	0.53±0.003	29.54	-4.21	29.66	-4.09	23.2	3.9	82	Y
ZS95	00:03:16.49	-29:58:47.4	12.38±0.003	0.93±0.005	0.90±0.007	28.92	-4.49	29.25	-4.16	20.1	2.7	60	Y
ZS91	00:03:20.61	-29:49:22.8	11.25±0.002	0.61±0.003	0.52±0.003	29.47	-4.29	29.40	-4.36	22.1	2.5	95	Y
ZS96 [†]	00:03:21.85	-30:01:10.5	10.32±0.001	0.48±0.001	0.39±0.001	29.50	-4.62	29.50	-4.61	20.8	3.5	92	Y
BLX-42 [§]	00:03:22.73	-29:53:50.5	16.50±0.104	2.28±0.109	...	29.41	-2.97	29.43	-2.96	23.0	7.4	02	Y
ZS94	00:03:24.18	-29:56:22.9	14.98±0.025	1.55±0.030	1.30±0.083	28.73	-3.89	29.13	-3.48	22.3	3.3	79	Y
ZS90	00:03:24.39	-29:48:49.4	10.62±0.001	0.54±0.002	0.45±0.001	29.57	-4.44	29.73	-4.27	20.7	3.5	90	Y
ZS93	00:03:24.67	-29:55:14.7	14.18±0.013	1.21±0.017	1.12±0.035	29.28	-3.53	29.44	-3.37	22.2	2.4	83	Y
ZS104	00:03:31.89	-29:43:04.8	10.05±0.001	0.46±0.001	0.36±0.001	29.75	-4.47	22.8	3.0	95	Y

Table 1—Continued

ID ^a	RA ^b [HH:MM:SS]	DEC ^b [DD:MM:SS]	V_0^c	$(V - I_c)_0^c$	$(B - V)_0^c$	ROSAT [0.1-2.4 keV]		XMM-NEWTON [0.3-5.0 keV]		$\mu_\alpha \cos \delta^e$	μ_δ^e	P_μ^e	P.M. ^e Mem.
						$\text{Log} L_x^d$	$\text{Log} L_x/L_{bol}$	$\text{Log} L_x^d$	$\text{Log} L_x/L_{bol}$				
PMS04-70	00:03:39.79	-30:02:09.5	11.37±0.002	0.58±0.003	0.49±0.003	28.59	-5.12	-4.9	-4.6	00	N
ZS107 ^{††}	00:03:50.17	-30:03:55.7	11.02±0.001	0.58±0.002	0.49±0.002	28.95	-4.88	22.0	2.9	97	Y
ZS115	00:04:12.57	-29:58:02.5	14.88±0.024	1.79±0.027	1.46±0.092	29.99	-2.84	21.7	4.3	70	Y
ZS134	00:04:49.20	-30:00:52.9	11.09±0.001	0.57±0.002	0.49±0.002	29.78	-4.04	23.4	5.0	29	Y
ZS138	00:04:58.84	-30:09:41.6	11.47±0.002	0.64±0.003	0.56±0.003	29.34	-4.34	22.4	2.6	95	Y
ZS142	00:05:04.93	-30:19:39.2	15.60±0.045	2.77±0.046	1.42±0.159	29.69	-3.29	99.1	1.2	00	N
BLX-62	00:05:07.01	-30:04:29.3	14.78±0.021	0.74±0.034	0.57±0.037	29.26	-3.10	8.7	-6.8	00	N
ZS144	00:05:07.08	-29:59:25.7	15.26±0.032	1.77±0.037	1.28±0.103	29.55	-3.12	21.8	5.0	33	Y
ZS148	00:05:14.39	-29:54:23.8	12.35±0.003	0.90±0.005	0.84±0.006	29.48	-3.91	22.8	4.0	87	Y
ZS154 [‡]	00:05:31.58	-30:20:51.6	13.42±0.007	1.07±0.010	0.96±0.016	29.56	-3.46	22.0	2.2	84	Y
ZS165 [†]	00:05:35.53	-29:57:06.4	12.50±0.003	...	0.85±0.007	29.41	-3.93	21.0	3.8	89	Y
ZS170	00:05:54.72	-30:06:25.8	12.07±0.003	0.74±0.004	0.69±0.005	29.17	-4.29	22.0	2.5	94	Y
BLX-79	00:05:58.13	-30:11:09.0	16.63±0.112	2.19±0.119	...	28.94	-3.36	27.5	-5.8	00	N
ZS172	00:06:04.29	-30:02:11.9	15.88±0.058	1.86±0.064	...	29.07	-3.39	21.3	3.2	49	Y
BLX-81	00:06:04.73	-29:57:06.7	15.74±0.051	0.92±0.076	0.92±0.117	29.33	-2.74	0.4	-12.8	00	N
ZS182	00:06:16.35	-30:05:57.1	11.66±0.002	0.68±0.004	0.61±0.004	29.27	-4.34	21.7	3.0	96	Y
ZS184	00:06:23.70	-29:52:04.7	15.58±0.049	2.91±0.050	...	29.75	-3.31	38.2	-78.1	00	N

^aNaming convention is as follows: ZS from de Epstein & Epstein (1985), BLX from M99 and, PMS04 from P04.

^bCoordinates are taken from the optical counterpart given in J09 and are J2000.

^cIntrinsic vales are derived using $E(B - V) = 0.016$ and $E(V - I_c) = 0.02$.

^dDistance used for luminosity calculation is 240 parsecs (see §3.1); unabsorbed luminosities are in erg s^{-1} .

^eProper motions and probabilities are taken from Platais et al. (2009); proper motions are in mas yr^{-1} .

^fMembership based on new proper motions. Y=proper motion member, N=proper motion non-member, NA=not available due to limiting magnitude of proper motion survey.

^gIdentical optical counterparts that are identified as two separate X-ray sources in M99 and P04 (see Table 2).

[†]isted as single-line spectroscopic binary in Mermilliod et al. (2008).

^{††}isted as double-line spectroscopic binary in Mermilliod et al. (2008).

[‡]isted as a single-line spectroscopic binary in Jeffries & James (1999).

Table 2. Multiple X-ray Source Detection to Single Optical Counterparts

ID	ROSAT		ID	XMM-NEWTON		Optical Counterpart	
	RA	DEC		RA	DEC	RA	DEC
ZS44	0:02:14.5	-29:48:58.6	PMS04-182	00:02:14.6	-29:49:03.5	00:02:14.65	-29:49:04.41
ZS60	0:02:41.8	-29:58:53.7	PMS04-97	00:02:41.7	-29:58:55.8	00:02:41.73	-29:58:53.19
BLX-12	0:02:07.2	-30:04:41.8	PMS04-48	00:02:07.6	-30:04:44.4	00:02:07.65	-30:04:42.90
BLX-15	0:02:22.3	-30:02:52.0	PMS04-66	00:02:22.7	-30:02:52.3	00:02:22.87	-30:02:52.88
BLX-16	0:02:23.1	-29:50:34.5	PMS04-169	00:02:23.4	-29:50:40.4	00:02:23.58	-29:50:39.99
BLX-42	0:03:22.3	-29:53:49.4	PMS04-150	00:03:22.6	-29:53:52.2	00:03:22.73	-29:53:50.89

Note. — Coordinates are J2000.0 Equinox.

Table 3. Mean values of L_x for Blanco 1

Spectral Range ^a	Mean $\text{Log}(L_x)$ [erg s ⁻¹]	1σ [erg s ⁻¹]
ROSAT - $B - V$		
G and Earlier	29.52	0.21
K	29.66	0.30
M and Later	29.61	0.52
ROSAT - $V - I_c$		
G and Earlier	29.57	0.22
K	29.65	0.33
M and Later	29.23	0.21
XMM:Newton - $B - V$		
G and Earlier	29.60	0.31
K	29.86	0.37
M and Later	29.69	0.40
XMM:Newton - $V - I_c$		
G and Earlier	29.62	0.33
K	29.76	0.47
M and Later	29.41	0.33

^aSpectral ranges are defined by Kenyon & Hartmann (1995): G-type and Earlier $B - V_0 < 0.8$, K-type $0.8 < B - V_0 < 1.3$, M-type and later $B - V_0 > 1.3$

Note. — X-ray luminosities were measured over the energy ranges of 0.1-2.4 keV and 0.3-5.0 keV for ROSAT and XMM-Newton, respectively.

Table 4. L_x and L_x/L_{bol} for Several Open Clusters

Name	Reference Number ^b	# of Stars Included	$\text{Log}(\text{Age})$ [yr]	Mean $\text{Log}(L_x)$ [erg s ⁻¹]	Mean $\text{Log}(L_x/L_{bol})$
G Spectral Type and Earlier ^a					
NGC 2547	1	22	7.48	29.71±0.46	-4.30±0.73
IC 2602 ^c	2	9	7.56
IC 2391	3	20	7.56	29.76±0.51	-4.64±1.14
α Persei	4	30	7.72	29.72±0.49	-3.67±0.57
Blanco 1 ^d	5	11	7.90	29.60±0.28	-4.29±0.24
Pleiades	6	31	8.08	29.44±0.36	-3.94±0.41
NGC 2516	7	54	8.15	29.40±0.42	-4.63±0.56
M 7	8	47	8.35	29.52±0.30	-4.32±0.32
Hyades	9	94	8.80	28.98±0.32	-4.96±0.60
Praesepe	10	36	8.86	29.18±0.38	-4.82±0.53
K Spectral Type ^a					
NGC 2547	1	23	7.48	29.92±0.37	-3.38±0.30
IC 2602	2	16	7.56	29.67±0.43	-3.54±0.30
IC 2391	3	13	7.56	29.87±0.22	-3.32±0.15
α Persei	4	51	7.72	29.67±0.42	-3.27±0.38
Blanco 1 ^d	5	25	7.90	29.71±0.40	-3.32±0.24
Pleiades	6	40	8.08	29.44±0.29	-3.21±0.29
NGC 2516	7	81	8.15	29.30±0.47	-3.77±0.55
M 7	8	56	8.35	29.42±0.32	-3.55±0.44
Hyades	9	42	8.80	28.83±0.53	-4.52±0.81
Praesepe	10	12	8.86	29.40±0.43	-4.10±0.78
M Spectral Type and Later ^a					
NGC 2547	1	52	7.48	29.42±0.32	-3.06±0.31
IC 2602	2	27	7.56	29.15±0.27	-3.27±0.29
IC 2391 ^c	3	4	7.56
α Persei	4	50	7.72	29.24±0.33	-2.89±0.34
Blanco 1 ^d	5	11	7.90	29.33±0.27	-3.16±0.24
Pleiades	6	43	8.08	29.16±0.20	-2.90±0.23
NGC 2516	7	90	8.15	28.97±0.31	-2.98±0.34
M 7 ^b	8	4	8.35
Hyades	9	48	8.80	28.84±0.36	-3.31±0.40
Praesepe	10	20	8.86	29.09±0.28	-3.11±0.47

^aSpectral ranges are defined by Kenyon & Hartmann (1995): G-type and Earlier $B - V_0 < 0.8$, K-type $0.8 < B - V_0 < 1.3$, M-type and later $B - V_0 > 1.3$

^bThe letters that come after the following citations represent -X XMM-Newton[0.3-10 keV] and -R ROSAT[0.1-2.4 keV]. *References:*(1)Jeffries et al. 2006-X, (2)Randich et al. 1995-R, (3)Patten & Simon 1996-R,(4)Randich et al. 1996-R, (5)Our new analysis, (6)Stauffer et al. 1994; Micela et al. 1999b-R, (7)Pillitteri et al. 2006-X, (8)Prosser et al. 1995-R, (10)Stern et al. 1995-R.,Perryman et al. 1998, (9)Randich & Schmitt 1995-R (*N.B.:* These reference numbers are also used in Fig. 8.)

^cDid not include mean L_x or L_x/L_{bol} values due to insufficient X-ray detections in mass ranges.

^dFor stars observed with ROSAT and XMM-NEWTON, we use the mean values in the calculations.